Structural and mechanistic classification of uronic acid-containing polysaccharide lyases

Garron, Marie-Line; Cygler, Miroslaw

Publisher's version / Version de l'éditeur:
https://doi.org/10.1093/glycob/cwq122
Glycobiology, 20, 12, pp. 1547-1573, 2010-08-30

Glycobiology vol. 20 no. 12 pp. 1547–1573, 2010
doi:10.1093/glycob/cwq122
Advance Access publication on August 30, 2010

REVIEW

Structural and mechanistic classification of uronic acid-containing polysaccharide lyases

Marie-Line Garron[2], and Miroslaw Cygler[1,2,3]

[2]Department of Biochemistry, McGill University, 3655 Promenade Sir William Osler, Montreal, Quebec, Canada H3G 1Y6; and [3]Biotechnology Research Institute, NRC, 6100 Royalmount Avenue, Montreal, Quebec, Canada H4P 2R2

Received on June 1, 2010; revised on August 6, 2010; accepted on August 11, 2010

Polysaccharide lyases (PLs) have been assigned to 21 families based on their sequences, with ~50 singletons awaiting further classification. For 19 of these families, the structure of at least one protein is known. In this review, we have analyzed the available structural information and show that presently known PL families belong to six general folds. Only two general catalytic mechanisms have been observed among these PLs: (1) metal-assisted neutralization of the acidic group of the sugar next to the cleaved bond, with, rather unusually, arginine or lysine playing the role of Brønsted base and (2) neutralization of the acidic group on the sugar by a close approach of an amino or acidic group forcing its protonation and Tyr or Tyr-His acting as the Brønsted base and acid.

Keywords: polysaccharide lyases/glycosaminoglycans/classification/enzymatic mechanism/fold analysis

Introduction

Carbohydrates are a large class of essential molecules common to all organisms. They are found most abundantly as polymers, either as oligo- or polysaccharides, usually linked to proteins or lipids. Carbohydrates possess a multiplicity of chiral centers and a large number of specific modifications, including acetylation, methylation, oxidation, and sulfonation, creating great chemical diversity from simple carbohydrate building blocks (Gabius 2000; Bertozzi and Kiessling 2001; Cummings and Stephen 2007). Polysaccharides are polymers formed of carbohydrate repeating units joined by glycosidic bonds. These are predominantly linear polymers but may contain various degrees of branching. Polysaccharides are essential cellular components of all living organisms and play multiple biological roles (Gagneux and Varki 1999; Schaefer and Schaefer 2010). They are involved in various cellular processes, including signal transmission (Mythreye and Blobe 2009; Schaefer and Schaefer 2010), immune response (Chen et al. 2008; Marth and Grewal 2008), bacterial pathogenesis (Boneca 2005), and cancer progression (Vlodavsky et al. 2007; Iozzo et al. 2009). Polysaccharides are most frequently found on cell surfaces in uni- and multicellular organisms (Gabius 2006) and in the extracellular matrix of higher eukaryotes (Iozzo 1998) and are essential components of cell wall of plants (Knox 2008; Sarkar et al. 2009). Within the extracellular matrix, they fulfill architectural functions providing elasticity (Knudson and Knudson 2001; Scott 2003) and serve as storage for many growth factors and other proteins (Macri et al. 2007). They form the building blocks of cell walls, providing physical rigidity and protection against the environment. Oligosaccharides are utilized for signaling during protein folding (Parodi 2000) and decorate many secreted proteins (Ohtsubo and Marth 2006). Many of these biologically important polysaccharides contain uronic acid within their repeating units.

Not surprisingly, all organisms contain a large number of enzymes dedicated to polysaccharide synthesis, modification, and degradation (Lairson et al. 2008). Some bacteria and plants relay on polysaccharides as a carbon source and contain an unusually large contingent of such enzymes (e.g. commensal *Bacteroides thetaiotaomicron*). The up-to-date classification of enzymes that degrade, modify, or create glycosidic bonds is maintained in the Carbohydrate Active enZYmes (CAZy) database (http://www.cazy.org/) (Cantarel et al. 2009). Carbohydrate modifying enzymes are divided into four classes: glycoside hydrolases (GHs), glycosyltransferases (GTs), polysaccharide lyases (PLs), and carbohydrate esterases (CEs). The structure and mechanisms of GHs and GTs have been extensively studied and frequently reviewed, most recently in (Henrissat et al. 2008). On the other hand, only limited reviews of specific families of PLs have been published (Jenkins et al. 1998; Hashimoto et al. 2005; Linhardt et al. 2006). The purpose of this review is to analyze and compare the structural and mechanistic features of PLs and to classify them based on their fold and catalytic mechanism.

Two chemical reactions are predominantly utilized for enzymatic depolymerization of polysaccharide chains: hydrolysis and lytic β-elimination (Yip and Withers 2004). Hydrolysis proceeds through the addition of a water molecule to break the glycosidic bond, creating a new reducing end on one fragment, with either retention or inversion of the configuration at C-1, and a saturated hexose ring on the nonreducing end of the other fragment (McCarter and Withers 1994). β-Eliminative

[1]To whom correspondence should be addressed: Tel: +1-514-496-6321; Fax: +1-514-496-5143; e-mail: mirek@bri.nrc.ca

cleavage of a glycosidic bond can occur when the sugar is substituted with an acidic group next to the carbon forming the glycosidic bond and results in the formation of a reducing end on one fragment and an unsaturated ring on the nonreducing end of the second fragment. The chemical steps of this mechanism were proposed by Gacesa (1987). Glucan polysaccharides can also be degraded by phosphorolysis by such enzymes as α-glucan phosphorylases (Withers et al. 1981). Eukaryotic enzymes that depolymerize polysaccharides predominantly utilize hydrolytic mechanisms while the lytic mechanism is found in many enzymes of bacterial or fungal origin as well as in plants and algae. In this review, we will discuss only PLs.

PLs act on polysaccharides containing a hexose oxidized at C-5 position to a carboxylic group and use β-elimination mechanism to cleave the glycosidic bond at the C-4 position. Three chemical steps have been proposed to occur during the β-elimination reaction (Figure 1A) (Gacesa 1987). First, the carboxyl group of the substrate is neutralized, often by a nearby positive charge, to reduce the p*K*a of the C-5 proton. Second, an enolate anion intermediate is created by proton abstraction at C-5. Then, electron transfer occurs from the carboxyl group to form a double bond between C-4 and C-5 with concomitant cleavage of the C-4–O-1 glycosidic bond. This bond cleavage creates two chemically distinct ends; the sugar on the new nonreducing end is unsaturated and contains a double bond between C4 and C5, while the sugar on the new reducing end remains saturated. Depending on the configurations at C-4 and C-5, the abstracted proton and the C-4 bridging oxygen can be either on the same side (*syn* configuration) or opposite sides (*anti* configuration) of the uronic acid ring. According to commonly used nomenclature (Davies et al. 1997), the sugars are numbered +1, +2, etc. from the cleavage site toward the reducing end and −1, −2, etc. toward the nonreducing end.

All identified PLs are classified into families within the CAZy database (http://www.cazy.org/) based on recognizable sequence homologies. They are presently divided into 21 families (1 to 22, family 19 has been moved to glycosyl hydrolases, Table I), with ~50 sequences as yet unclassified. The number of families is expected to grow with the rapid progress in sequencing of new genomes through many large-scale sequencing efforts (http://www.ncbi.nlm.nih.gov/sites/entrez?db=genome). Within the last several years, the three-dimensional structures of many PLs have been determined, allowing extension of the evolutionary relationships between these proteins beyond what was possible to deduce from sequence analysis alone. Presently, 19 of 21 PL families have a known three-dimensional structure of at least one representative (Table I). Only two families, PL12 and PL17 have as yet unassigned folds. Of these, heparan sulfate (HS) lyase family PL12 is the largest without a representative structure.

Polysaccharide substrates bind to their respective lyases along an extended surface on the enzyme, with several consecutive sugars making contacts with the protein. The sites on the enzyme surface interacting with individual sugars are termed "subsites" and are given numbers according to the position of the sugar they interact with, as described above. Therefore, the enzyme's substrate-binding site is divided into $+n$ and $-n$ subsites (n = 1,2,3,...), with cleavage occurring between sugars located in the +1 and −1 subsites. In the majority of PL enzymes, the subsites −2 to +2 are the most important determinants of substrate specificity.

In this review, we analyze the available data on the structure and catalytic mechanisms of PLs and group the PL families into classes based on their folds.

Substrates of PLs

PL substrates have different origins: bacterial, plant, or animal. Nevertheless, they present relatively similar chemical structures composed of repetitive blocks of pyranoses. Each block is composed of two to five saccharides linked by a (1-4) glycosidic bond. PLs described here require an acidic group at +1 sugar. Based on the nature of the +1 sugar, the substrates of PLs can be divided into three groups: (1) galacturonic acid, (2) glucuronic/iduronic acid, and (3) mannuronate/guluronate. Polysaccharides in the first group include pectate and pectin, the second group includes hyaluronan, chondroitin, chondroitin sulfate (CS), dermatan sulfate (DS), heparin, HS, heparosan, glucuronan, and xanthan, and the third group contains alginates.

Pectin/pectate (galacturonate)

Pectate/pectin is the common term to indicate the structural acidic polysaccharide from the cell wall of higher plants (Roberts 1990; Cosgrove 1997; Ridley et al. 2001). This polymer is widely used in the food industry as a gelling and thickening agent or stabilizer. Based on the carbohydrate components and their degree of modification, two types of polysaccharide regions are distinguished: the "smooth" region containing predominantly polygalacturonan (PGA) and the "hairy" region that contains rhamnogalacturonan I and II (RG I, RG II). The PGA contains α-1,4-linked GalA sugars that can be partially 6-*O*-methylated and acetylated at C-2 and/or C-3 positions (Ridley et al. 2001) (Figure 1B). The RG I and RG II in the hairy regions are highly modified on the L-rhamnose (Rha) and also partially acetylated at the C-2 and C-3 positions of GalA (Ridley et al. 2001). The enzymes degrading PGA are designated pectate or pectin lyases. Pectin lyases are mainly synthesized by fungi and act on less negatively charged, highly methylated pectins, whereas bacterial pectate lyases (Pels) degrade highly negatively charged non-methylated or low-esterified substrates and cleave α-1,4 linkages between galacturonosyl residues. Generally, Pels require Ca^{2+} ions for activity and have an optimal pH in the basic range. The exceptions are Pels from family PL2, which preferentially utilize Mn^{2+} ions. Contrary to Pels, pectin lyases have optimal pH around 5.5 and do not require metal ions for activity. Pectin and pectate lyases have been classified within six PL families, PL1, PL2, PL3, PL9, PL10, and PL22. These enzymes are predominantly endolytic and extracellular (Abbott and Boraston 2008); no structure of an exolytic pectate lyase has so far been determined.

Contrary to pectate lyases, enzymes cleaving the RG I regions have been less well studied. Rhamnogalacturonan lyases (RLs) act specifically on [2)-α-L-Rha-(1-4)-α-D-GalA (1] bonds of the RG I main chain. The C-4-Rha is usually a branch point where arabinan, galactan, and arabinogalactan are attached, creating the "hairy" region. This branching influences the extent of degradation, for example deacetylation or

A

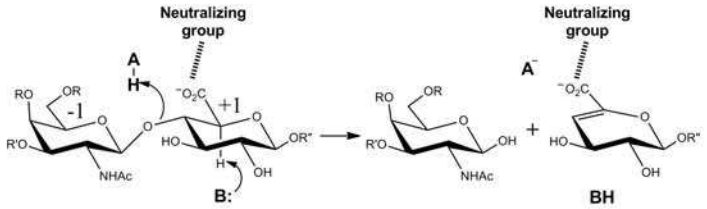

B

Pectate/Pectin

Polygalacturonic acid: [4)-α-D-GalA-(1-4)-α-D-GalA(1]$_n$

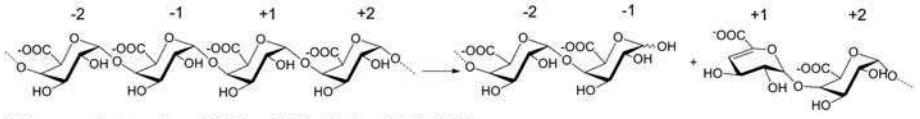

Rhamnogalacturonic acid: [2)-α-L-Rha-(1-4)-α-D-GalA(1]$_n$

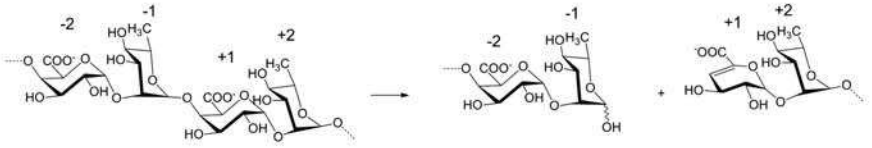

Heparin [4)-α-L-IdoA2S-(1-4)-α-D-GlcNS6S(1]$_n$

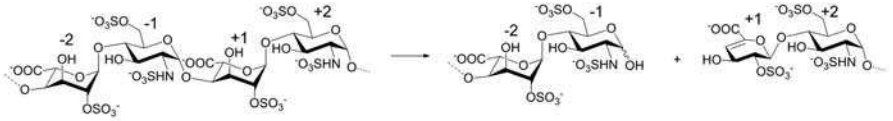

Heparan sulfate [4)-β-D-GlcA-(1-4)-α-D-GlcNY6X(1]$_n$, X = H, SO_3^-, Y = $COCH_3$, SO_3^-

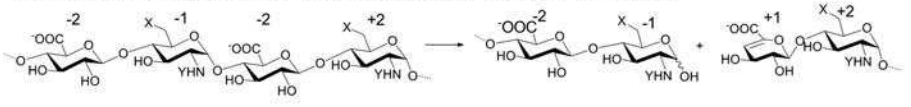

Heparosan [4)-β-D-GlcA-(1-4)-α-D-GlcNCOCH$_3$(1]$_n$

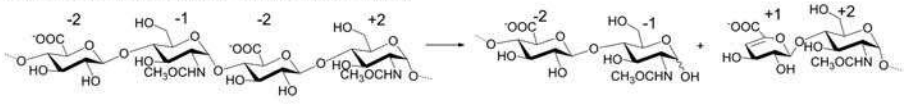

Chondrotin sulfate A [4)-β-D-GlcA-(1,3)-β-D-GalNAc4S(1]$_n$

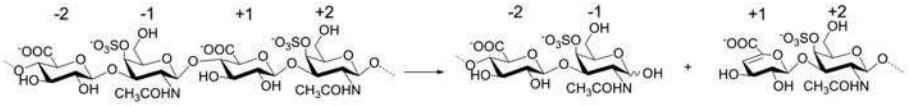

Chondrotin sulfate C [4)-β-D-GlcA-(1,3)-β-D-GalNAc6S(1]$_n$

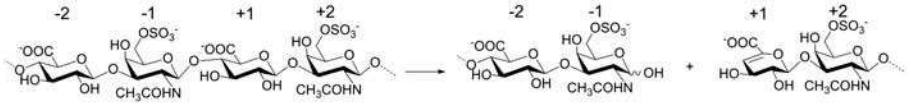

Chondrotin [4)-β-D-GlcA-(1,3)-β-D-GalNAc(1]$_n$

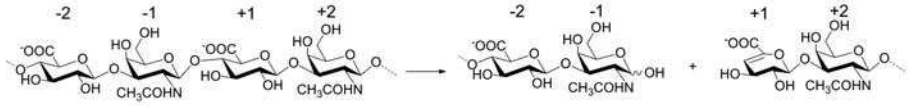

Dermatan sulfate [4)-α-L-IdoA-(1,3)-β-D-GalNAc4S(1]$_n$

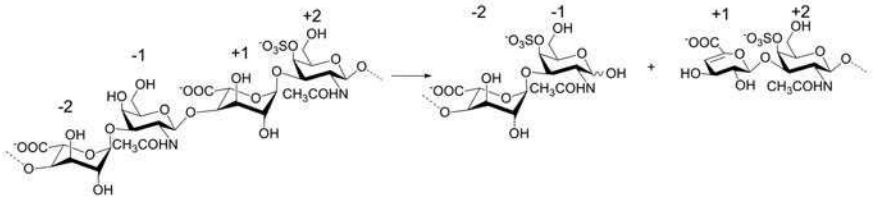

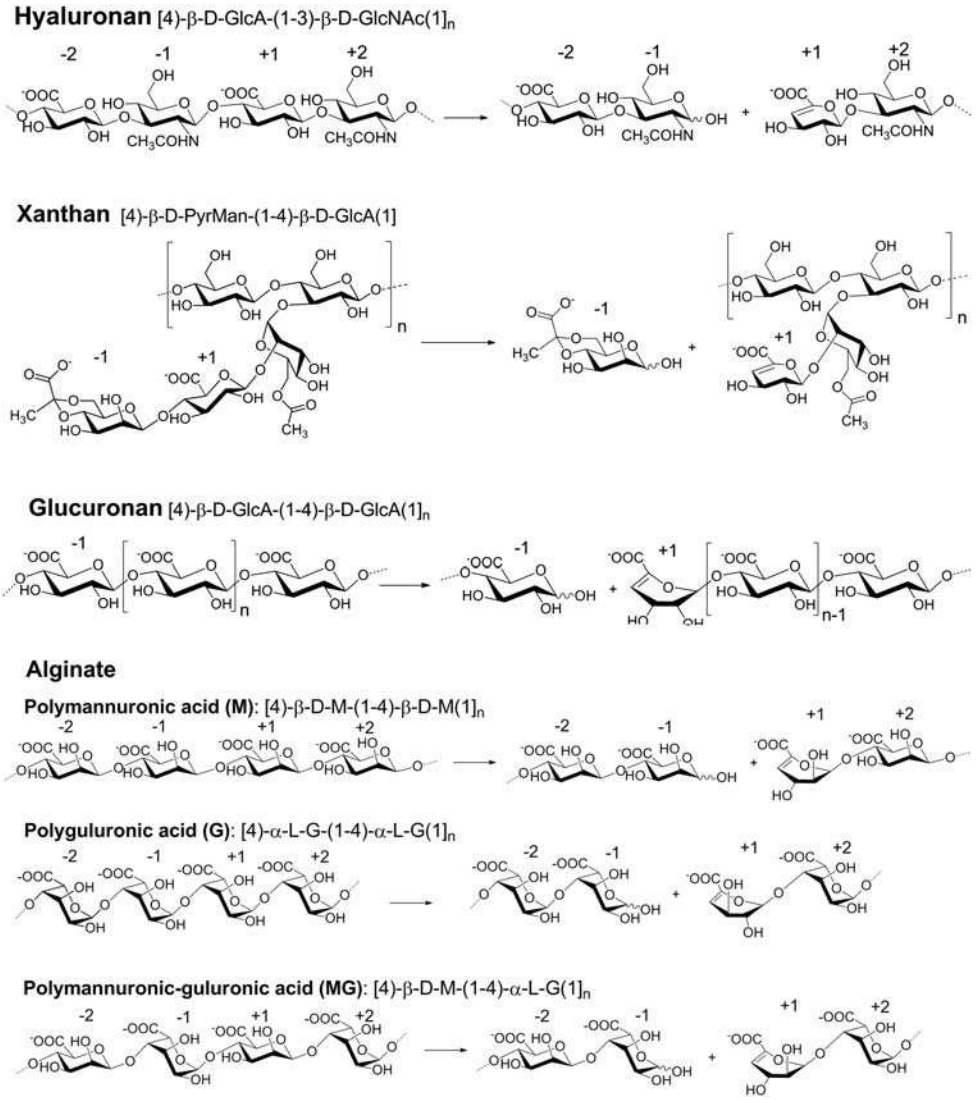

Fig. 1. (**A**) General mechanism of β-elimination reaction; (**B**) substrates of polysaccharide lyases and products of the cleavage reaction.

reduction of arabinan sidechains increases enzymatic activity (Mutter et al. 1998). RLs are classified into two families, PL4 and PL11, which are mainly comprised of fungal and bacterial enzymes, respectively. A bacterial RG degradation pathway has been recently described in *Bacillus subtilis* strain 168, containing two PL11 RLs, an exolytic and an endolytic, participating together in the degradation of the RG I region (Ochiai, Itoh, Kawamata et al. 2007).

Polysaccharides containing glucuronic/iduronic acid

A large group of PL substrates in this class are glycosaminoglycans (GAGs). They are linear anionic polysaccharides, mainly of eukaryotic origin. Their disaccharide repeating units contain a hexosamine linked 1-4 to an uronic acid. GAGs, with the exception of hyaluronic acid (HA), are *O*-linked to core proteins via a serine residue, forming proteoglycans, which are involved in the regulation of various cellular processes such as cell adhesion, signaling, cell proliferation, or inflammation. GAGs such as heparin, HS, heparosan, chondroitin sulfate, chondroitin, DS, and HA are substrates of PLs. GAG lyases are produced by various bacteria that can use the resulting mono- and disaccharides as a carbon source. They are classified as members of families PL6, PL8, PL12, PL13, PL16, and PL21. In addition to GAGs, two other polysaccharides are found that contain glucuronic acid: xanthan and glucuronan. Xanthan is degraded by xanthan lyases (XLs) belonging to the PL8 family, while glucuronan is degraded by glucuronan lyases belonging to the PL14 and PL20 families.

HS and Heparin. HS and heparin are negatively charged, linear polysaccharides, composed of repeating disaccharide units made up of uronic acid and glucosamine residues (GlcN, 2-amino-2-deoxy-α-D-glucopyranose) (Esko and Selleck 2002) (Figure 1B). HS has a diverse primary structure and is characterized by a high percentage of the GlcA (β-D-glucopyranosyluronic acid). Both GlcA and its minor C-5 epimer, iduronic acid (IdoA, α-L-idopyranosyluronic acid) can be infrequently sulfated at the

Table I. Polysaccharide lyase families with associated activities and assigned fold

PL	Enzyme activity	EC	Fold
1	Pectate lyase Exo-pectate lyase Pectin lyase	4.2.2.2 4.2.2.9 4.2.2.10	β-Helix (10 turns)
2	Pectate lyase Exo-pectate lyase	4.2.2.2 4.2.2.9	$(\alpha/\alpha)_7$ Toroid
3	Pectate lyase	4.2.2.2	β-Helix (8 turns)
4	Rhamnogalacturonan lyase	4.2.2.-	3 β-Sandwich domains
5	Alginate lyase	4.2.2.3	$(\alpha/\alpha)_4$ Incomplete toroid
6	Alginate lyase Chondroitinase B	4.2.2.3 4.2.2.4	β-Helix (14 turns)
7	Alginate lyase α-L-Guluronate lyase	4.2.2.3 4.2.2.11	β-Jelly roll
8	Chondroitinase AC Xanthan lyase Hyaluronate lyase Chondroitinase ABC	4.2.2.5 4.2.2.12 4.2.2.1 4.2.2.20	$(\alpha/\alpha)_{5,6}$ Incomplete toroid + antiparallel β-sandwich + N-terminal antiparallel β-sandwich
9	Pectate lyase Exopolygalacturonate lyase	4.2.2.2 4.2.2.9	β-Helix (11 turns)
10	Pectate lyase	4.2.2.2	$(\alpha/\alpha)_3$ Incomplete toroid
11	Rhamnogalacturonan lyase	4.2.2.-	β-Propeller (eight-bladed)
12	Heparinase III	4.2.2.8	N.D.
13	Heparinase I	4.2.2.7	β-Jelly roll
14	Alginate lyase Exo-oligo-alginate lyase β-1,4-Glucuronan lyase	4.2.2.3 4.2.2.- 4.2.2.14	β-Jelly roll
15	Oligo-alginate lyase	4.2.2.-	$(\alpha/\alpha)_{5,6}$ Incomplete toroid + antiparallel β-sandwich
16	Hyaluronan lyase	4.2.2.1	Triple-stranded β-helix
17	Alginate lyase	4.2.2.3	N.D.
18	Alginate lyase	4.2.2.3	β-Jelly roll
19	Endo-β-1,4-glucuronan lyase	4.2.2.14	β-Jelly roll
20	Heparinase II Archan-sulfate lyase	4.2.2.7/8 4.2.2.-	$(\alpha/\alpha)_{5,6}$ Incomplete toroid + antiparallel β-sandwich
21	Oligogalacturonan lyase		β-Propeller (seven-bladed)
NC	K5 lyase (heparosan lyase)	4.2.2.-	Triple-stranded β-helix

C-2 position. The GlcN is frequently *N*-acetylated (GlcNAc) and, to a limited extent, sulfated at the C-2, C-3, and *N*-positions. The modifications in HS are concentrated within specific regions of the polysaccharide, known as the high S domains, giving rise to short sequence motifs responsible for the interactions between HS and a diverse repertoire of proteins leading to its multiple biological roles. HS-GAGs are abundant at the cell surface as part of proteoglycan cell surface receptors (Jackson et al. 1991; Kjellen and Lindahl 1991).

Heparin has a high content (~90%) of IdoA that is frequently sulfated at the C-2 position (Linhardt 2003). The glucosamine residue in heparin is predominantly substituted with *N*-sulfo groups (GlcNS), with only a small number of *N*-acetyl groups and 6-*O*-sulfo groups, as well as rare 3-*O*-sulfo groups. Cleavage of the heparin GAG chain is an important part of its biological activity, which leads to the release of heparin-binding proteins, e.g. various growth factors, as well as the creation of short-specific oligosaccharides that regulate hemostasis through

interactions with proteins of the blood coagulation cascade (Capila and Linhardt 2002; Munoz and Linhardt 2004).

Four types of bacterial heparin/HS lyases have been identified. Heparinase I (HepI) is specific for heparin and cleaves the bond on the nonreducing end of iduronic acid, heparinase III (HepIII) cleaves HS at the nonreducing end of glucuronic acid, while heparinase II (HepII) can depolymerize both heparin and HS. These enzymes have been classified to three different PL families. HepI belongs to the PL13 family, HepIII to PL12, and HepII was recently assigned to a new family, PL21. Heparosan K5 lyase is an *E. coli* phage enzyme that cleaves the unsulfated bacterial polysaccharide heparosan (the biosynthetic precursor to heparin and HS) and HS next to GlcA but is intolerant of sulfated polysaccharides (Rek et al. 2007).

Chondroitin and DSs. CS and DS are major components of cartilage, blood vessels, and tendons (Yoon and Halper 2005; Roughley 2006). CS is widely used as a dietary supplement and is believed to be beneficial in the treatment of osteoarthritis due to its anti-inflammatory action (Lauder 2009) and, together with DS, has potential for applications in regenerative medicine and in the treatment of viral infections (Yamada and Sugahara 2008). CS and DS are composed of disaccharide repeating units of α/β-D-uronate-(1,3)-β-D-*N*-acetylgalactosamine (GalNAc) (Figure 1B). CS contains the C-5 epimer GlcA while DS contains the IdoA (Ernst et al. 1995). Five types of CS are distinguishable based on their sulfation pattern: CS-A contains sulfate at the C-4 position, CS-B (now known as DS) is sulfated at C-4, CS-C is sulfated at C-6, CS-D is sulfated at C-2 and C-6, and CS-E is sulfated at C-4 and C-6. Additional sulfation can occur at the C-2 position of IdoA and at the C-6 position of GalNAc in DS. Chondroitin, lacking sulfate groups, is the biosynthetic precursor of both CS and DS and is synthesized by commensal and pathogenic bacteria (DeAngelis et al. 2002).

As is the case with heparinases, several types of bacterial chondroitin lyases have been identified differing in substrate specificity (Linhardt et al. 2006). Chondroitin lyase AC (ChonAC) degrades CS-A and C, chondroitin lyase B (ChonB) is specific for DS, and chondroitin lyase ABC (ChonABC) shows broad specificity and can cleave CS-A/C and DS. The ChonAC and ChonABC enzymes belong to the PL8 family while ChonB belongs to the PL6 family.

Hyaluronan. Hyaluronan (HA) is a long, unsulfated polysaccharide synthesized directly in the plasma membrane, rather than in the Golgi like other GAGs. Abundant in higher organisms, HA is present in tissues such as skin, cartilage, or neural tissue (McDonald and Camenisch 2002; Kogan et al. 2007). Due to its wide distribution, HA is used in various medical applications including eye surgery, osteoarthritis, and tissue engineering. Some bacteria and viruses synthesize capsular HA that allows them to evade the host immune system (DeAngelis 2002). HA is composed of repeating units of [3)-β-D-*N*-acetylglucosamine-(1,4)-β-D-GlcA-(1] (Figure 1B). This disaccharide block is similar to that found in CS, and HA lyases (HLs) also show some activity toward CS. Bacterial HLs are similar in sequence to ChonAC and ChonABC and belong to the same PL8 family. Bacteriophage invading *Streptococcus* strains also produces enzymes with HL activity but unrelated sequence. These HLs are also found in some *Streptococcus* strains and have been classified within the PL16 family.

Xanthan. Xanthan is an extracellular hetero-polysaccharide synthesized by the pathogenic bacterium, *Xanthomonas campestris*. Xanthan is a common food additive used for its ability to increase viscosity of liquids. It is composed of a branched pentasaccharide repeat unit, in which the disaccharide, β-D-glucose-(1,4)-β-D-glucose, forms the main chain polymer. The second disaccharide's glucose is substituted at the C-3 position by a trisaccharide [β-D-mannose-(1,4)-β-D-glucuronic acid-(1,2)-β-D-mannose-(1,3] (Figure 1B) (Garcia-Ochoa et al. 2000). Both mannose units can be acetylated at the C-6 position and a pyruvate can be added on C-4 or C-6 position via a ketal linkage (Hashimoto et al. 1998). XL specifically degrades the link [β-D-mannose-(1,4)-β-D-glucuronic acid] on the branched section. So far, only two xanthan lyases from *Bacillus* sp. GL1 and *Paenibacillus alginolyticus* XL-1 have been characterized (Hashimoto et al. 1998; Ruijssenaars et al. 2000). Like the majority of lyases cleaving the glycosidic bond next to GlcA, xanthan lyase belongs to the PL8 family.

Glucuronan. Glucuronan is a less abundant polysaccharide, synthesized by some bacteria, fungi, and algae. This polysaccharide is of interest to the food and pharmacological industries for its rheological and biological properties. It is composed of (1,4) linked β-D-glucuronic acids and is partially acetylated at the C-3 and/or C-2 positions (Figure 1B) (Miyazaki et al. 1975; Heyraud et al. 1993; Redouan et al. 2009). Glucuronan is the first example of a homoglucuronic acid polymer synthesized by bacteria. Several glucuronan lyases have been identified and are classified within families PL14 and PL20.

Alginate (mannuronate)

Alginate is a linear polysaccharide produced by some bacteria belonging to the *Pseudomonas* and *Azotobacter* genera and by brown seaweed (Fischer and Dorfel 1955; Rehm and Valla 1997). It contains α-L-guluronate (G) or its C-5 epimer, β-D-mannuronate (M), connected by (1-4) linkages (Figure 1B). In *Pseudomonas* species, this polysaccharide plays a role in virulence related to alginate-mediated biofilm formation that helps to avoid phagocytosis (Russell and Gacesa 1989; Pritt et al. 2007). Alginate from brown seaweed is widely used in the food and pharmaceutical industries for its capacity to chelate ions and for its gelling properties. Three distinct regions can be found along the alginate chain, the homopolymeric poly(M), poly(G) blocks and an alternate poly(MG) block. Poly(M) bacterial alginate is more frequently acetylated at the C-2 and/or C-3 position of mannuronate than alginate from seaweed (Remminghorst and Rehm 2006). Accordingly, various bacterial strains contain lyases that can degrade these polysaccharides. Alginate lyases have been found within several PL families, namely in PL5, PL6, PL7, PL14, PL15, PL17, and PL18.

PL fold classes

At the time of writing, 19 out of 21 PL families have at least one structural representative. The structures show that the number of folds observed among PL enzymes is smaller than the number of families and indicate distant evolutionary relationships between several families, which could not be detected from their sequences alone. We have organized the PL families into six general folds and classified PLs accordingly into classes (Table II).

Table II. Fold classes and PL families associate with each class

Class		PL family	Enzyme	Substrate
β-Helix		PL1	Pectate/pectin lyase	PGalA
		PL3	Pectate lyase	PGalA
		PL9		
		PL6	Chondroitinase B	DS
β-Jelly roll		PL7	Alginate lyase	Poly(G), poly(M), poly(MG)
		PL14		
		PL18		
		PL13	Heparinase I	Heparin
		PL20	Glucuronate lyase	PGlcA
$(\alpha/\alpha)_n$ Toroid	$(\alpha/\alpha)_7$ Toroid	PL2	Pectate lyase	PGalA
	$(\alpha/\alpha)_3$ Incomplete toroid	PL10	Pectate lyase	PGalA
	$(\alpha/\alpha)_4$	PL5	Alginate lyase	Poly(G), poly(M), poly(MG)
	$(\alpha/\alpha)_{5,6}$ Incomplete toroid + β-sandwich	PL8	Chondroitinase AC	CS-A, CS-C, HA
			Chondroitinase ABC	CS-A, DS, CS-C
			Xanthan lyase	Xanthan
			Hyaluronate lyase	HA
		PL15	Oligo-alginate lyase	Poly(G), poly(M), poly(MG)
		PL21	Heparinase II	Heparin/HS
β-Sandwich		PL4	Rhamnogalacturonan lyase	RG I, PGalA
β-Propeller	Eight-bladed	PL11	Rhamnogalacturonan lyase	RG I, PGalA
	Seven-bladed	PL22	Oligogalacturonan lyase	PGalA
Triple-stranded β-helix		PL16	Hyaluronan lyase	HA

Polygalacturonic acid (PGalA); polyglucuronic acid (PGlcA); dermatan sulfate (DS); polyguluronate (Poly(G)); polymannuronate (Poly(M)); chondroitin sulfate A and C (CS-A, CS-C); hyaluronic acid (HA); heparan sulfate (HS); rhamnogalacturonan I (RG I).

Right-handed β-helix class

The right-handed β-helix is the most abundant fold among PL families. Four families, PL1, PL3, PL6 and PL9, share this fold. PL1, PL3, and PL9 are pectate lyase families, PL6 contains alginate and DS lyases. PL1, with more than 400 assigned sequences and over 35 known three-dimensional structures, is the largest family of PLs and contains proteins from bacteria, plants, and fungi.

The right-handed β-helix was first observed in the structure of the pectate lyase C (PelC) from *Erwinia chrysanthemi* (Yoder et al. 1993) (Figure 2A). Each turn of this helical architecture is composed of three β-strands PB1, PB2, and PB3 connected by turns T1 (between PB1 and 2), T2 (PB2 and 3), and T3 (PB3 and 1) (Figure 2B). The β-strands are rather short, containing three to five residues with strands PB1 and PB2 being nearly antiparallel to each other. Proteins in this class contain from 8 to 14 helical turns, creating three parallel β-sheets extending along the helix axis (Jenkins et al. 1998). The T2 turns usually contain only two residues, with the second residue adopting the α_L conformation that introduces a 90° bend to the polypeptide backbone. The second T2 residue in consecutive turns is frequently an asparagine that forms the so called "asparagine ladder" (Yoder et al. 1993). The T3 turns are longer than T1 or T2 and can participate in the active site. With the exception of proteins with the fewest number of turns (eight turns), the N-terminal end of the β-helix is capped by an amphipathic α-helix preceding the first PB1 strand. The N-terminal and C-terminal extensions usually form irregular structures that pack against small hydrophobic patches on the PB2 and T2 sides of the β-helix, respectively. The inner part of the β-helix is lined with stacks of hydrophobic and aromatic residues. Sequence alignment of pectate lyases from the PL1 family shows that PB2, PB3, and T2 are the most conserved parts of the structure. The PB1 strands and T3 turns, involved in the substrate-binding site and contributing to the formation of the active site, show greater variability, adapting to the nature of their specific substrates.

The β-helix formed by members of the PL3 family differs somewhat from that found in other PL families. This is the shortest β-helix, with only eight turns and is devoid of the N-terminal capping α-helix (Figure 2C). An asparagine stack occurs at the first position of T2 turns, rather than at the second position observed in other families, and these sidechains are facing toward the exterior of the β-helix. No aromatic stacks are present inside the β-helix, and the rigidity of the structure is maintained by interactions of hydrophobic sidechains and disulfide bonds, five of which are present in PelI (P3B8Y), (Creze et al. 2008). Some of the enzymes from the PL3 family contain an additional fibronectin III-like domain that presumably mediates interactions with other protein(s) (Creze et al. 2008).

β-Jelly roll class

Five families of PLs, PL7, PL13, PL14, PL18, and PL20, share a β-jelly roll fold (Figure 3). The enzymes belonging to the β-jelly roll PL class degrade diverse polysaccharide substrates. Members of families PL7, PL14, and PL18 degrade alginate, PL13 depolymerize heparin, and PL20 break down glucuronate. In this structural family, PL7, PL13, and PL18 contain mainly bacterial enzymes, whereas PL14 contains viral en-

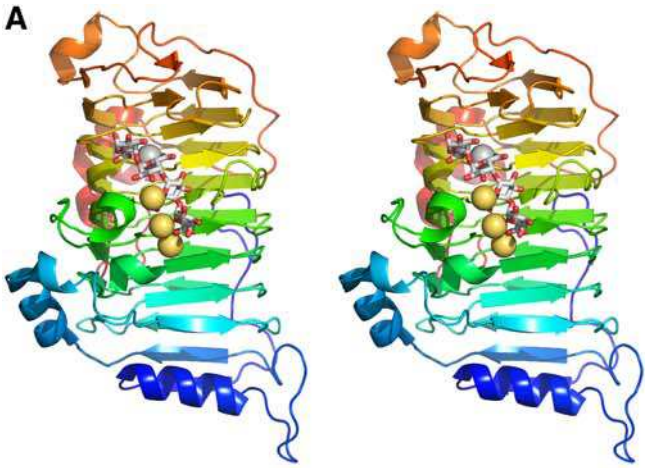

Right-handed β-helix fold (PDB code 2EWE)

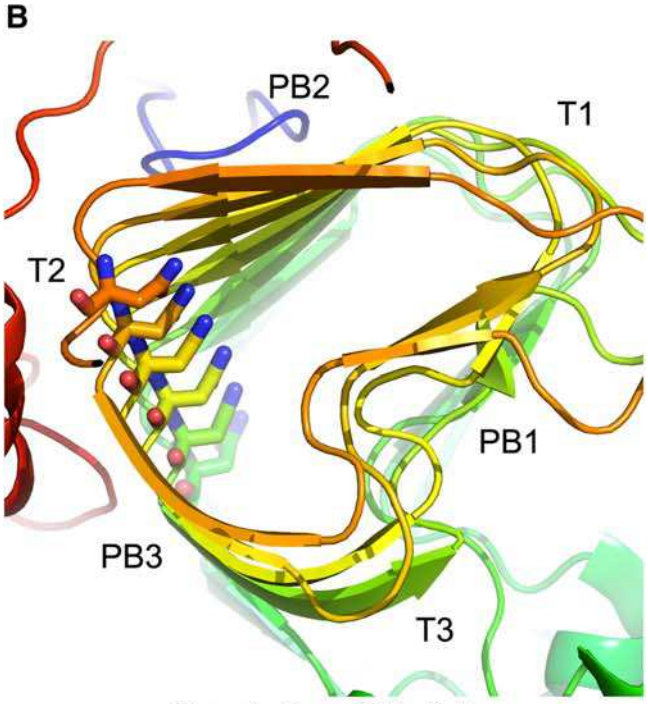

Organization of β-helix turns

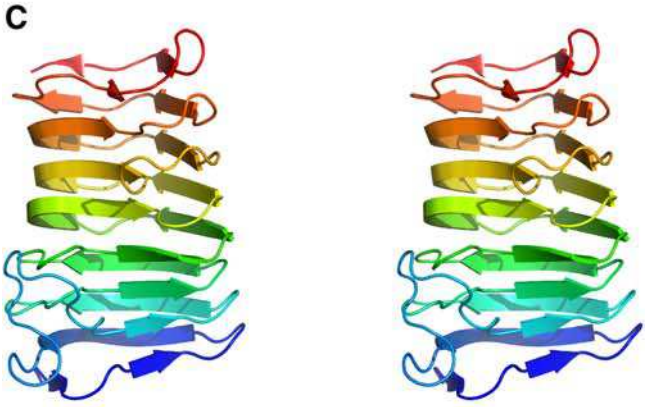

Short β-helix with eight turns (PDB code 1EE6)

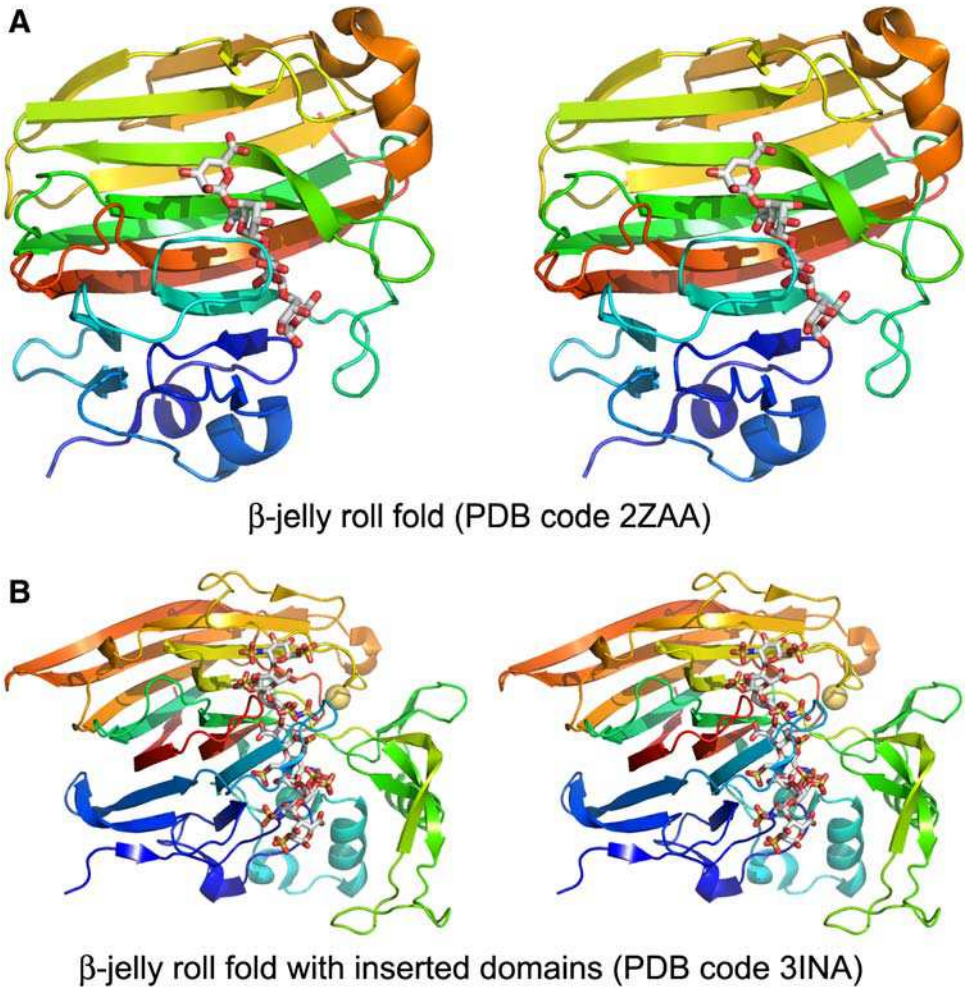

Fig. 3. The β-jelly roll fold. (**A**) The typical fold for enzymes from families PL7, PL13, and PL18 (PDB code 2ZAA); (**B**) the structure of PL13 HepI (PDB code 3INA) with small domains inserted into the canonical fold (green and cyan on the right). Bound oligosaccharides are shown in stick mode.

zymes and PL20 eukaryotic enzymes. The canonical fold is made up of two antiparallel seven-stranded β-sheets bent in the middle by nearly 90° (Yamasaki et al. 2004). The resulting curvature creates a groove in which the substrate binds and defines the location of the active site (Figure 3). Some enzymes with this fold have one or two additional strands in one or both sheets. The loops linking the inner and outer β-sheets are variable in length and sequence. In some structures, these loops are very short, e.g. in the family of PL7 alginate lyases, while in other structures they can be quite long and fold into independent domains. The largest proteins in this class are PL13 enzymes that have two additional extensions in the middle of the sequence (Figure 3B), e.g. the thumb domain in HepI (Han et al. 2009). The long loops are often rigidified by the presence of structural ions (Ca^{2+}), although these metal-binding sites are not conserved within the proteins of this class. In HepI, the Ca^{2+} ion binds on the side of the β-sandwich and joins two long loops that stabilize the base of the thumb domain (Han et al. 2009). In PL18, the Ca^{2+} ion is situated on the opposite side of the β-sheet compared to that in HepI (PDB code 1J1T, unpublished). This Ca^{2+} ion adds rigidity to a long loop. Finally, in PL20 enzymes, the Ca^{2+} ion is located at the top of the outer sheet, and it is involved in stabilization of the N-terminal end (Konno et al. 2009).

$(\alpha/\alpha)_n$ Toroid class

Several PL families contain a domain that is formed by a repetition of a pair of antiparallel α-helices (helical hairpin), with each helix composed of 10–20 residues. The hairpins are arranged counterclockwise (looking from the top of the hairpin). The number of hairpins, *n*, varies from three to seven. We classify these folds together within an $(\alpha/\alpha)_n$ toroid class. This class can be divided into several subclasses: single-domain $(\alpha/\alpha)_n$

Fig. 2. The right-handed β-helix fold drawn in a cartoon form. The polypeptide is rainbow colored, from blue at the N-terminus to red at the C-terminus. (**A**) The structure of the canonical pectate lyase PelC (PDB code 2EWE) with nine full turns of the β-helix. The three calcium ions with full occupancy are shown as yellow spheres, and the ion present only in the R218K mutant is shown in gray. Bound tetrasaccharide is shown in stick mode; (**B**) the view down the β-helix axis with strands PB1, PB2, and PB3 and turns T1, T2, and T3 marked explicitly. Residues forming the asparagine ladder in T2 are shown in a stick representation; (**C**) the structure of pectate lyase from *Bacillus* sp. strain ksm-p15 having the shortest, eight-turn β-helix and no additional extension (PDB code 1EE6). This and other figures were prepared with PyMOL (www.pymol.org).

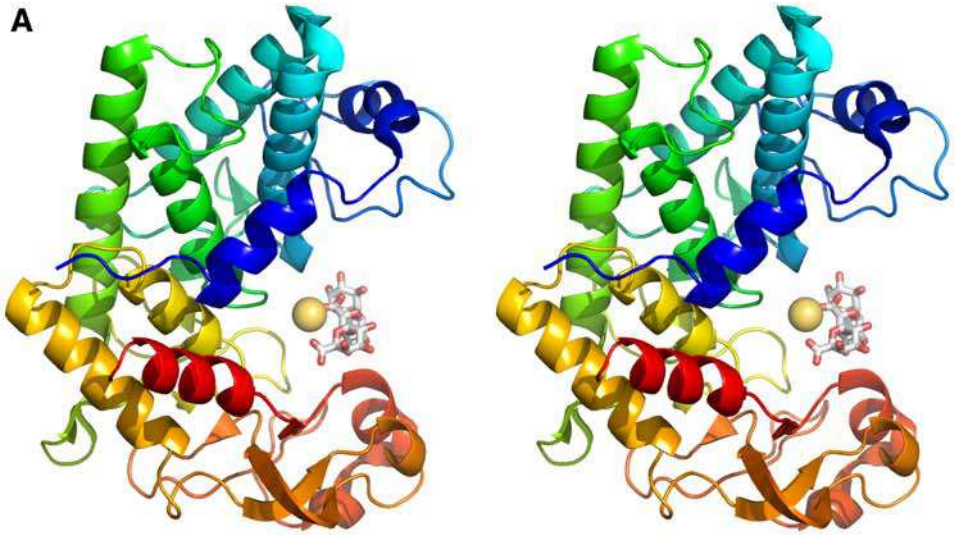

$(\alpha/\alpha)_3$ incomplete toroid (PDB code 1GXO)

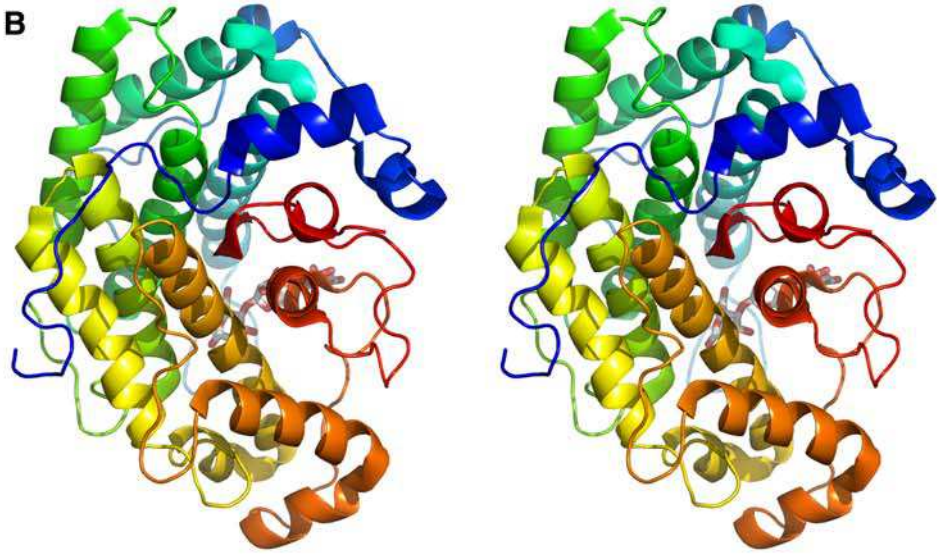

$(\alpha/\alpha)_4$ incomplete toroid (PDB code 1HV6)

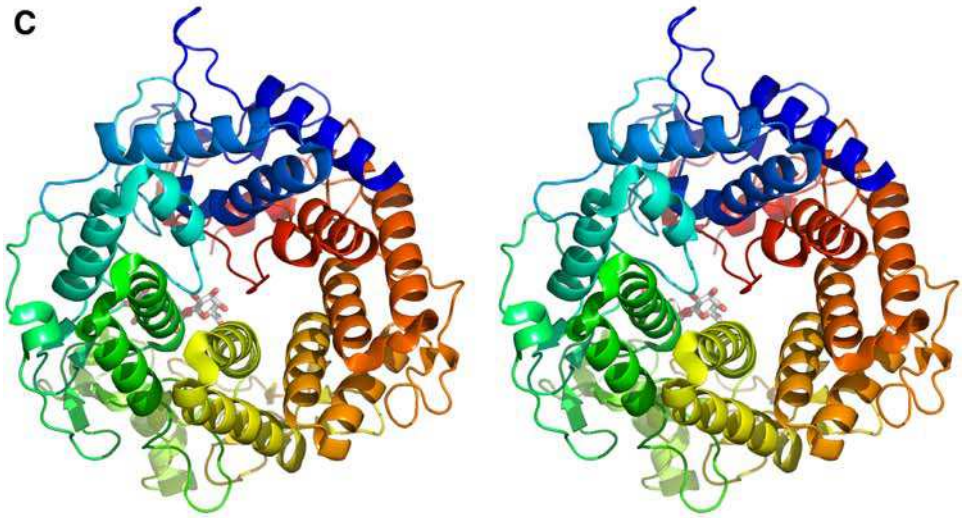

$(\alpha/\alpha)_7$ toroid (PDB code 2V8K)

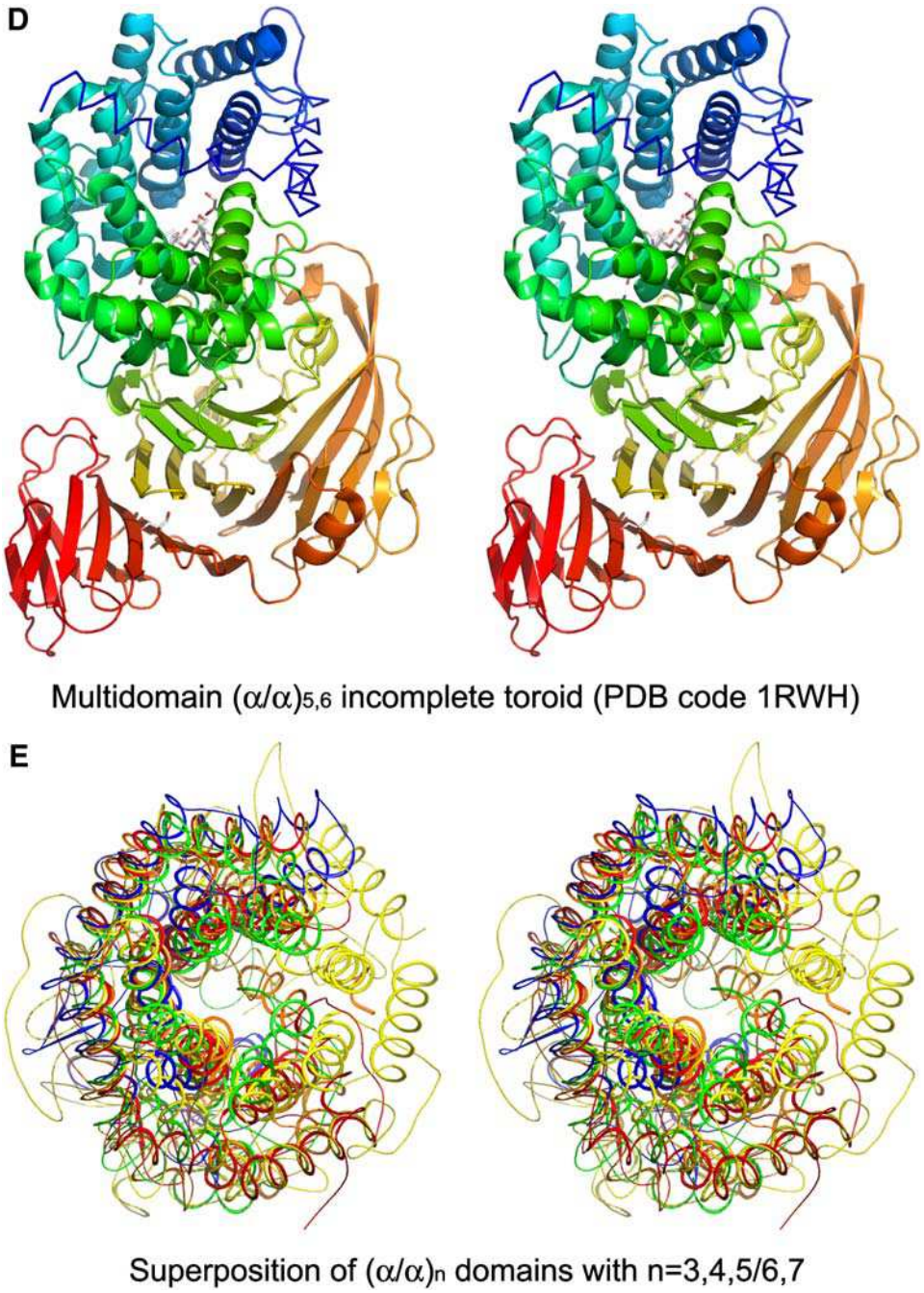

Fig. 4. The $(\alpha/\alpha)_n$ domain fold. (**A**) $(\alpha/\alpha)_3$ Incomplete toroid (PDB code 1GXO); (**B**) $(\alpha/\alpha)_4$ incomplete toroid (PDB code 1HV6); (**C**) $(\alpha/\alpha)_7$ toroid (PDB code 2V8K); (**D**) the multidomain $(\alpha/\alpha)_{5,6}$ incomplete toroid (PDB code 1RWH); (**E**) the superposition of these four folds showing good superposition of the first several α-helical hairpins. Colors: $(\alpha/\alpha)_3$ 1GXO (PL10)—blue, $(\alpha/\alpha)_4$ 1HV6 (PL5)—green, $(\alpha/\alpha)_{5,6}$ 1RWH (PL8)—red, $(\alpha/\alpha)_{5,6}$ 2FUT (PL21)—orange, and $(\alpha/\alpha)_7$ 2V8K (PL2)—yellow.

toroids with three, four, or seven α-helical hairpins and multiple domain proteins with $(\alpha/\alpha)_{5,6}$ toroid domain, a C-terminal domain composed of a β-sandwich of four antiparallel β-sheets and, frequently, an additional β-sheet N-terminal domain. The $(\alpha/\alpha)_7$ forms a full toroid while the structures with smaller number of hairpins form incomplete toroids. A characteristic feature of the α-helical hairpins is a short connection between the helices and significantly longer connections between the consecutive hairpins. In all cases, the substrate-binding sites are located on the side of these long connections, near the top of the (semi)-toroid. Despite different number of α-helical hairpins in various PL families, these structures can be superposed with reasonable root mean squares deviations, starting from the N-terminal hairpins.

The single-domain $(\alpha/\alpha)_n$ toroid subclasses encompass the PL2, PL5, and PL10 families. The PL10 family has only three hairpin repeats, $(\alpha/\alpha)_3$ (Charnock et al. 2002) (Figure 4A), alginate lyases from PL5 contain four hairpin repetitions,

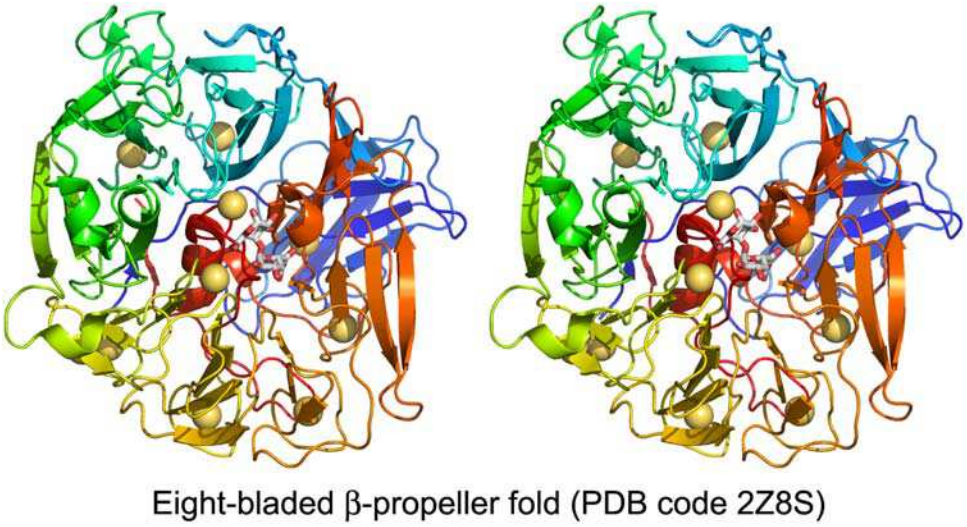

Fig. 5. The β-propeller fold. The eight-bladed propeller is preceded by a β-sheet domain (PDB code 2Z8S). The substrate (gray sticks) binds on the opposite end of the propeller domain to the N-terminal domain. Seven β-sheet blades are stabilized by Ca^{2+} ions (yellow spheres), and two additional Ca^{2+} ions bind near the substrate.

$(\alpha/\alpha)_4$ (Yoon et al. 2001) (Figure 4B), and PL2 has seven repeats, $(\alpha/\alpha)_7$ (Abbott and Boraston 2007) (Figure 4C). They differ somewhat in the curvature of the (semi)-toroid formed by the helical hairpins but the first several hairpins can be superimposed relatively well (Figure 4E).

The multidomain $(\alpha/\alpha)_{5,6}$ toroid subclass contains additional domains. The $(\alpha/\alpha)_{5,6}$ toroid domain contains five α-helical hairpins and in some proteins a sixth hairpin is assembled from two additional antiparallel helices, one at the N-terminus and the other at the C-terminus of this domain. This domain is followed by a C-terminal antiparallel β-sandwich domain containing four β-sheets (Féthière et al. 1999; Hashimoto et al. 2003) (Figure 4D). Some lyases, such as ChonABC and HL, contain also a small N-terminal β-sandwich domain (Li and Jedrzejas 2001; Huang et al. 2003; Shaya, Hahn, Bjerkan et al. 2008). In this subclass, the C-terminal domain

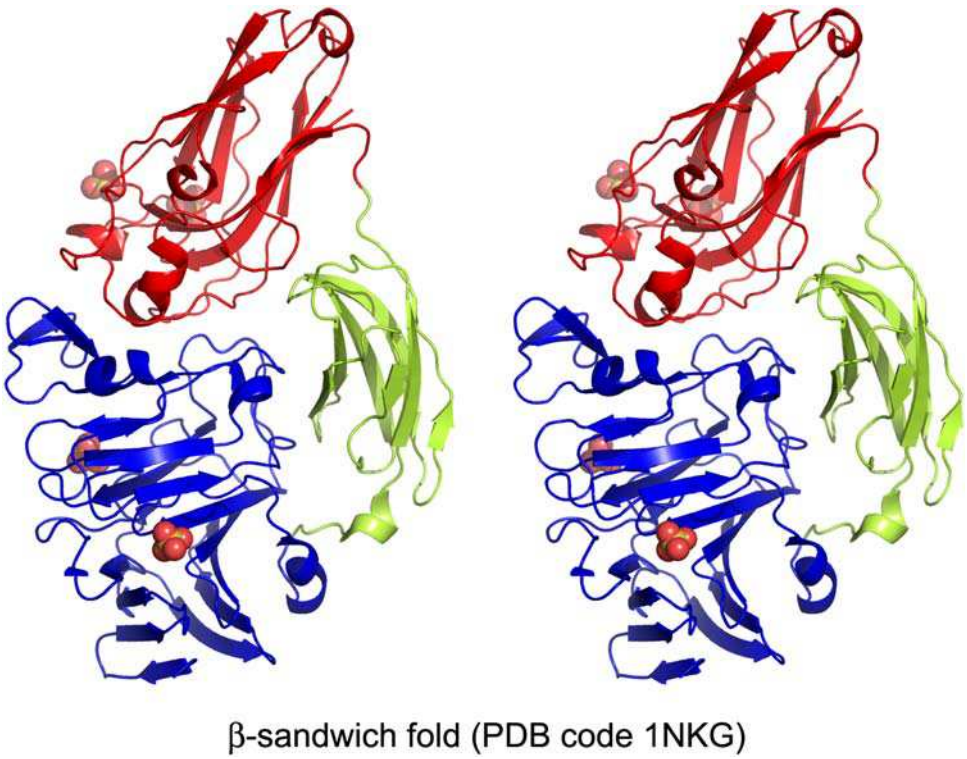

Fig. 6. β-Sandwich fold. The structure of PL4 rhamnogalacturonan lyase from *Aspergillus aculeatus* (PDB code 1NKG) contains three domains colored blue, green, and red, respectively. The active site is within the domain. The bound Ca^{2+} (yellow) and sulfate ions are shown explicitly as spheres.

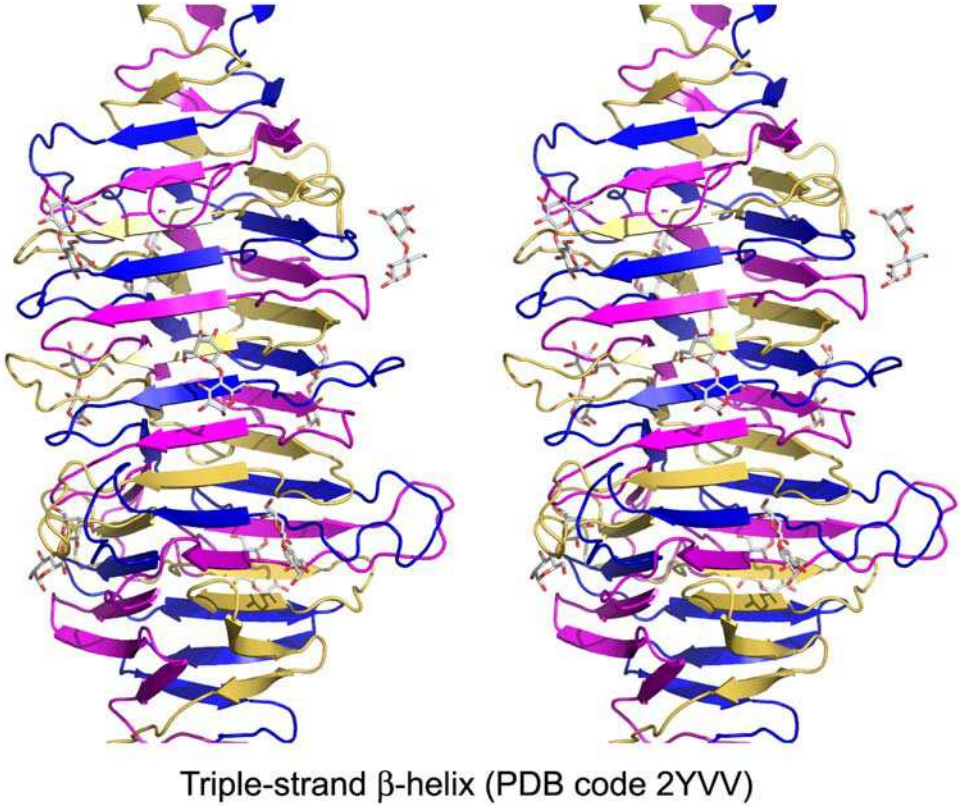

Fig. 7. Triple-stranded β-helix (PDB code 2YVV). The three intertwined subunits are shown in different colors: yellow, blue, and magenta. Bound disaccharides are shown in stick mode.

participates in the formation of the substrate-binding site and contributes one amino acid to the catalytic tetrad. The PL8 family belongs to this subclass and contains lyases that can depolymerize several different substrates: CS-A, -B, or -C, HA, and xanthan. All these enzymes, with exception of HLs, contain structural ions, calcium or sodium, coordinated mainly by aspartate sidechains. Despite similarities in their structures, none of these metal ion sites are conserved across this enzyme family. Apparently, these sites are not essential for maintaining this particular fold since their location is variable. For example, xanthan lyase from *Bacillus* sp. has a Ca^{+2} ion in the native structure (PDB code 1J0M) and no ion in the complex with mannose (PDB code 2E22) (Hashimoto et al. 2003; Maruyama et al. 2007).

Two other small families share with PL8, the multidomain $(\alpha/\alpha)_{5,6}$ toroid subclass, namely PL15 and PL21. The PL15 family contains bacterial oligo-alginate or exotype alginate lyases. The structure of the first enzyme from this family was determined recently (PBD code 3AFL) (Ochiai et al. 2010). Structural comparison shows that PL15 lyase is more similar to family PL21 than to PL8 lyases. Like ChonABC and hyaluronan lyases, this alginate lyase possesses a small β-sandwich domain at the N-terminus, but its orientation differs from those in the ChonABC and hyaluronan lyases. A structural ion is also found in this family. A potential chloride ion links the N-terminal helical domain to the C-terminal β-sandwich but like for PL8 this ion is not essential (Ochiai et al. 2010). The PL21 family contains HepII enzymes. Like other PLs from this subclass, HepII contains a structural ion (zinc) that links several long loops in the C-terminal β-sandwich domain (Shaya et al. 2006).

β-Propeller class

The lyases from two PL families display β-propeller fold, PL11 and PL22. *B. subtilis* RG PL11 lyases YesW and YesX differ in their mode of action: YesW is an endolytic enzyme while YesX is an exolytic enzyme (Ochiai, Itoh, Maruyama et al. 2007). Both enzymes share the same fold and their exo/endo specificity is linked to the presence of an extended loop in the exolytic YesX that blocks polysaccharide binding on the "−" side (Ochiai et al. 2009). Both enzymes are composed of two domains. The N-terminal domain contains two three-stranded antiparallel β-sheets and is followed by an eight-bladed β-propeller domain (Figure 5). Each blade contains four antiparallel β-strands and each blade, except for blade D, contains a structural Ca^{2+} ion. One end of the propeller is occluded by the N-terminal domain and is plugged by the C-terminal α-helix. The substrate binds to the opposite open end of the β-propeller (Figure 5).

The oligogalacturonate lyase from *Vibrio parahaemolyticus* (PDB code 3C5M, F. Forouhar et al., unpublished) is a seven-bladed β-propeller with no additional domains. In contrast to PL11 lyases, no structural ions are present; however, one Mn^{2+} ion is located at the entrance to the deep depression at one end of the propeller, presumably the location of the substrate-binding site.

Among the carbohydrate processing enzymes, the β-propeller fold is not limited to PLs but is also found among GHs. For ex-

Table III. Catalytic residues of PLs

	Fold	$(\alpha/\alpha)_{5,6}$ Toroid + β-sandwich						β-Jelly roll				$(\alpha/\alpha)_4$
	PL family	PL8				PL15	PL21	PL7	PL13	PL18	PL20	PL5
	Enzyme	ChonAC	XL	HL	ChABC	Oligo-alg L	HepII	Alg L	HepI	Alg L	Gluc L.	Alg L
	PDB code[a]	1RWH	1JON	1I8Q	2Q1F	3AFL	2FUT	1UAI	3IKW	1J1T	2ZZJ	1HV6
	+1 Substrate	GlcA	GlcA	GlcA	GlcA/IdoA	G/M	GlcA/IdoA	G/M	IdoA	G/M	GlcA	M
	anti- base				His345	His311[b]	His202	His119	His151	His92	Ile93	His192
	anti- acid				Tyr461	Tyr365[b]	Tyr257	Tyr195	Tyr357	Tyr186		Tyr246
Catalytic tetrad	*syn*- base/acid	Tyr242	Tyr255	Tyr488	Tyr461	Tyr365[b]	Tyr257				Tyr200	
		His233	His246	His479	His454	His531[b]	His406	Arg72	Arg83	Arg52	His53	Arg239
		Arg296	Arg309	Arg542	Arg514							
		Glu407	Glu421	Glu657	Glu628							
	Neutralizer	Asn183	Asn196	Asn429	Asp398	Arg314[b]	Glu205	Gln117	Gln149	Gln90	Gln91	Asn191
								Glu74	Glu85	Glu54	Glu55	Glu236

[a]Representative structure.
[b]To be confirmed.

ample, the 6-bladed β-propeller fold occurs in family GH33 while five blades are observed in family GH62 (CAZy database (Cantarel et al. 2009)).

β-Sandwich class

The structure of the PL4 family of RLs has no structural similarity with RLs from the PL11 family or with any other lyases. While PL11 contains essential bacterial sequences, the PL4 family mainly comprises eukaryotic enzymes of fungal and plant origin. The only structural representative with this fold in PL4 is the eukaryotic RL from *Aspergillus aculeatus* (McDonough et al. 2004). The *A. aculeatus* lyase contains three domains (Figure 6). The N-terminal domain is the largest and is predicted to contain the catalytic site. The central and C-terminal domains are presumed to be involved in binding the polysaccharide substrate. These domains were identified as a fibronectin type III-like domain and a carbohydrate binding module-like domain, respectively. The N-terminal β-sandwich domain is formed from two antiparallel eight-stranded β-sheets (McDonough et al. 2004).

Triple-stranded β-helix

The triple-stranded β-helix is found in bacteriophage tail spike proteins (TSPs) that are essential for phage virulence. The three strands are intertwined to form a single β-helix or fold independently into three β-helices when the chains are held together through the interactions of N- and/or C-terminal domains. Some TSPs possess catalytic activity to degrade polysaccharides of the bacterial envelope. Example of glycosidases include endo-α-L-1,3-rhamnosidase from *Salmonella* phage P22 and from family GH90 (PDB code 1TSP (Steinbacher et al. 1994)) and bacteriophage K1F endo-4,8-sialidase from family GH58 (PDB code 1VOF (Stummeyer et al. 2005)).

This fold is also found in PLs (hyaluronidase) from family PL16. The PL16 family of bacteriophage-encoded HL is found in the genomes of virulent *Streptococcus* species and in phages invading *Streptococcus*. The phage HL helps the phage to penetrate the capsule of its bacterial host by degrading the HA layer and reducing the capsule viscosity. These HLs are distinct from PL8 HLs not only in their fold but also in that they are specific for HA and cannot digest CS substrates. They are composed of three intertwined polypeptides forming a triple-

Table IV. Active site of metal-dependent lyases

Active site →	Isostructural					Similar	Different			
Fold	β-Helix				$(\alpha/\alpha)_3$ Toroid	$(\alpha/\alpha)_7$ Toroid	β-Helix	β-Propeller		
PL	PL1		PL3	PL9	PL10	PL2	PL6	PL11		PL22
Enzyme	Pel	Pectin lyase	Pel	Pel	Pel	Pel	ChB	RL		OligoGal.
PDB code[a]	2EWE	1QCX	3B8Y	1RU4	1GXO	2V8K	1OFL	2Z8S		3C5M
Neutralizer	1-2 Ca^{2+}	Arg176 (replaces Glu166)	Ca^{2+}	Ca^{2+}	Ca^{2+}	Mn^{2+}	Ca^{2+}	Ca^{2+}		Mn^{2+}
Metal stabilizers	Asp131, Glu166, Asp170		Asp173[b], Asp195[b], Glu194[b],	Asp209, Asp233, Asp234, Asp237	Asp451	Glu130, His109, His172	Glu243, Glu245, Asp213	Site 1 Asp153, Asn596	Site 2 His363, His399, Asp401, Glu422	His287, His353, His355, Gln350
Base	Arg218	Arg236	Lys224	Lys273	Arg524	Arg171	Lys250	Lys535[b] or Arg452[b],		Arg349[b]
Acid	H_2O	H_2O	H_2O	H_2O	H_2O	H_2O	Arg271	H_2O[b]		H_2O[b]

[a]Representative structure.
[b]To be confirmed.

Table V. Association between the substrate and mechanism. Families with no structural information are shown in italics

Substrate	Class	Mechanism	PL family
Heparin	β-Jelly roll	Tyr/His, Gln	PL13
	$(\alpha/\alpha)_5$ Toroid	Tyr/His, Glu	PL21
HS	$(\alpha/\alpha)_5$ Toroid	Tyr/His, Glu	PL21
	N.D. (Hep3)	*N.D.*	*PL12*
HA	$(\alpha/\alpha)_5$ Toroid	Tyr/His, Asn	PL8
	Triple-stranded β-helix	Tyr/Arg, Gln	PL16
CS	$(\alpha/\alpha)_5$ Toroid	Tyr/His, Asn	PL8
DS	β-Helix	Ca^{2+}	PL6
	$(\alpha/\alpha)_5$ Toroid	Tyr/His, Asp	PL8
Xanthan	$(\alpha/\alpha)_5$ Toroid	Tyr/His, Asn	PL8
Pectate	β-Helix	Ca^{2+}	PL1, PL3, PL9
	$(\alpha/\alpha)_{3,7}$ Toroid	Mn^{2+}, Ca^{2+}	PL2, PL10
	β-Propeller (seven-bladed)	Mn^{2+}	PL22
Pectin	β-Helix	Arg/Arg	PL1
Alginate	β-Jelly roll	Tyr/His, Gln	PL7, PL18
		N.D.	PL14
	β-Helix	Ca^{2+}	PL6
	$(\alpha/\alpha)_4$ Toroid	Tyr/His, Asn	PL5
	$(\alpha/\alpha)_{5,6}$ Toroid	Tyr/His, Arg	PL15
	N.D. (AlyII)	*N.D.*	*PL17*
Glucuronan	β-Jelly roll	Tyr, Gln	PL20
		N.D.	PL14
Rhamnogalacturonan	β-Sandwich	*N.D.*	PL4
	β-Propeller (eight-bladed)	Ca^{2+}	PL11

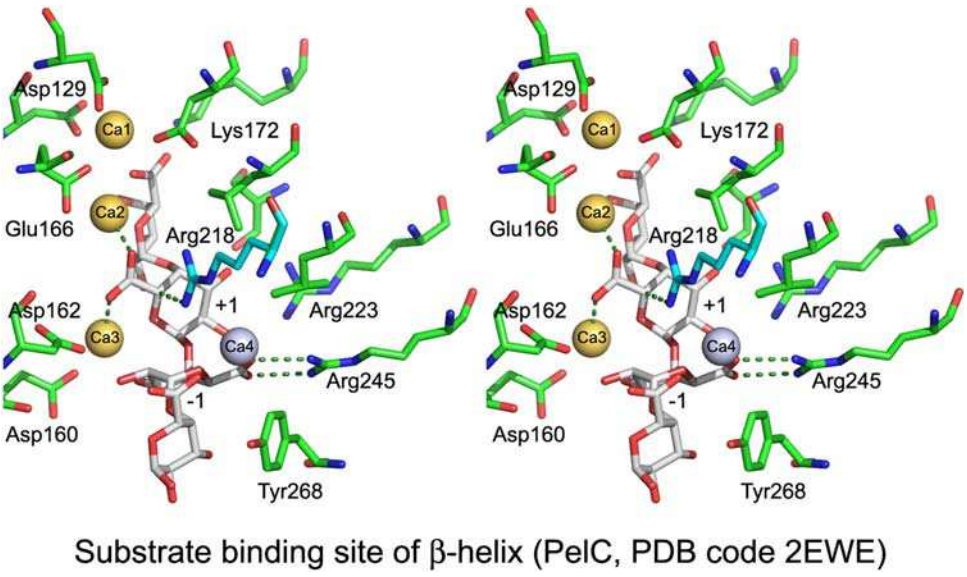

Fig. 8. The substrate-binding site of PelC with active site residues and calcium ions (PDB code 2EWE). The three most important Ca^{2+} ions are colored in yellow, the fourth (observed only in the R218K mutant) is gray. The position of Arg218 is modeled based on the native structure. The numbering of the Ca^{2+} ions corresponds to the references in the text. The key contacts are marked with dashed lines. The sugars on either side of the cleaved bond are marked "+1" and "−1".

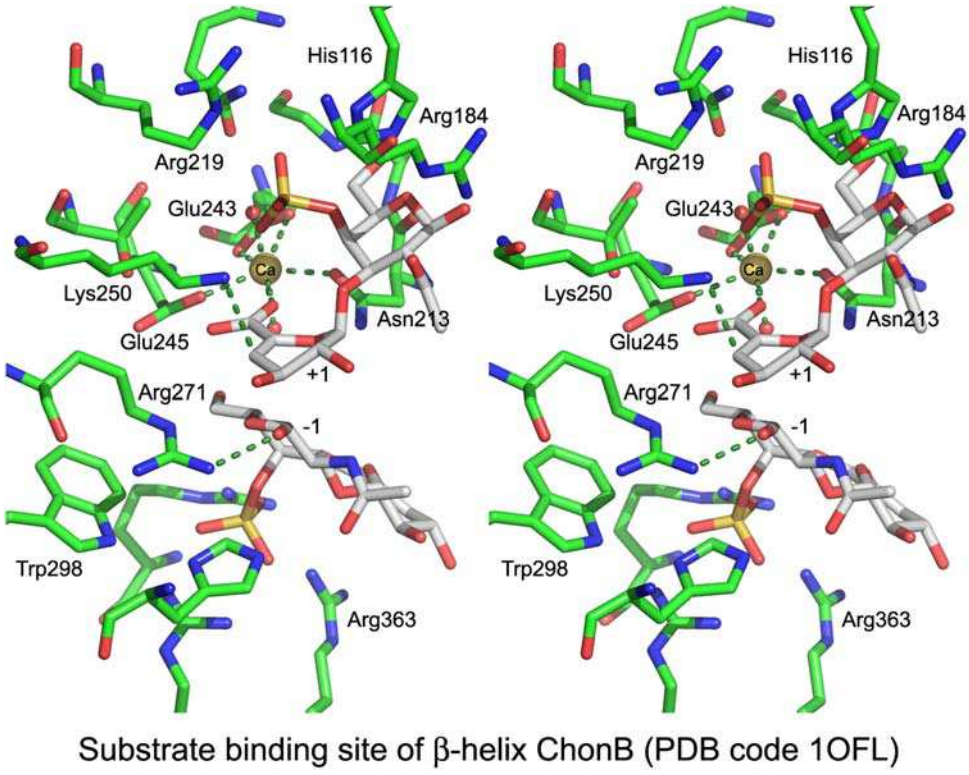

Fig. 9. The substrate-binding site of ChonB (PDB code 1OFL). The Ca^{2+} ion (yellow ball) neutralizes the acidic group of +1 sugar; Lys250 is proposed to act as the Brønsted base and Arg271 as the Brønsted acid. Relevant close contacts are marked with dashed lines.

stranded β-helix (Figure 7) (Smith et al. 2005; Mishra et al. 2009). The three polypeptide chains form an N-terminal α/β capping domain followed by two helical coiled-coil, a central right-handed β-helix in the shape of an irregular triangular tube and another coiled-coil. The β-strands of the central β-helix are bent, with their concave surface pointing outside the helix, which creates a depression along each side of the β-helix. This depression is the binding site for HA polysaccharide chains (Figure 7).

A TSP KflA from coliphage K5A is another example of a PL, which cleaves K5 capsular polysaccharide. This enzyme has not yet been assigned to a PL family due to the lack of sufficient sequence similarity to already classified enzymes. The structure shows that the three polypeptide chains are intertwined at the N- and C-terminal ends but in the central part the chains fold into individual β-helices (Thompson et al. 2010). This fold resembles more the GH90 than the PL16 family.

Active site topologies and catalytic mechanisms

The β-elimination reaction results in breaking the glycosidic bond adjacent to a carboxylate group to form a new reducing end and an unsaturated sugar at the nonreducing end. This process occurs in three steps: (1) neutralization of the C-5 carboxyl group that lowers the p*K*a of the H-5 proton and increases its susceptibility for abstraction, (2) proton abstraction leading to an enolate intermediate, and (3) elimination of the glycosidic bond with concomitant electron transfer from the carboxylate group to form a double bond between C-4 and C-5. The β-elimination reaction requires participation of a Brønsted base to accept the H-5 proton and a Brønsted acid to donate the proton to the leaving group recreating a new reducing end.

The crystal structures of PLs from various families, frequently with bound substrates or products, together with mutagenesis data, have in most cases allowed insight into the reaction mechanisms at the molecular level. These catalytic mechanisms fall into two general categories based on the nature of the group neutralizing the C-5 carboxyl and the residues playing the role of Brønsted base and acid (Figure 1A): (1) metal (Ca^{2+}, rarely Mn^{2+})-assisted neutralization of the acidic group, with Lys or Arg as a Brønsted base and a water molecule as a Brønsted acid or (2) neutralization of the acidic group by Asn/Gln or a protonated Asp/Glu, with Tyr or His as a Brønsted base and Tyr as a Brønsted acid. The available data (multiple crystal structures, sequence conservation of active site residues) strongly suggest that the type of enzymatic mechanism is conserved within each PL family (with some variability in the details, acquired during evolution). Our analysis shows that conservation of the enzymatic mechanism extends over the entire fold class (or a subclass in the case of $(\alpha/\alpha)_n$ toroid enzymes). Such conservation of mechanistic features provides additional support that there exists a common ancestry among the enzymes from the same class, extending beyond the recognized PL families. Moreover, several different fold classes share the same mechanism with sometimes surprising similarities of their active sites, indicating a convergent evolution of several different folds to adopt the same molecular solution to the problem of polysaccharide bond cleavage.

The metal ion-assisted mechanism is found in the β-helix class, $(\alpha/\alpha)_{3/7}$ classes, and β-propeller classes (Table III), while the Asx/Glx-assisted mechanism is found in the remaining clas-

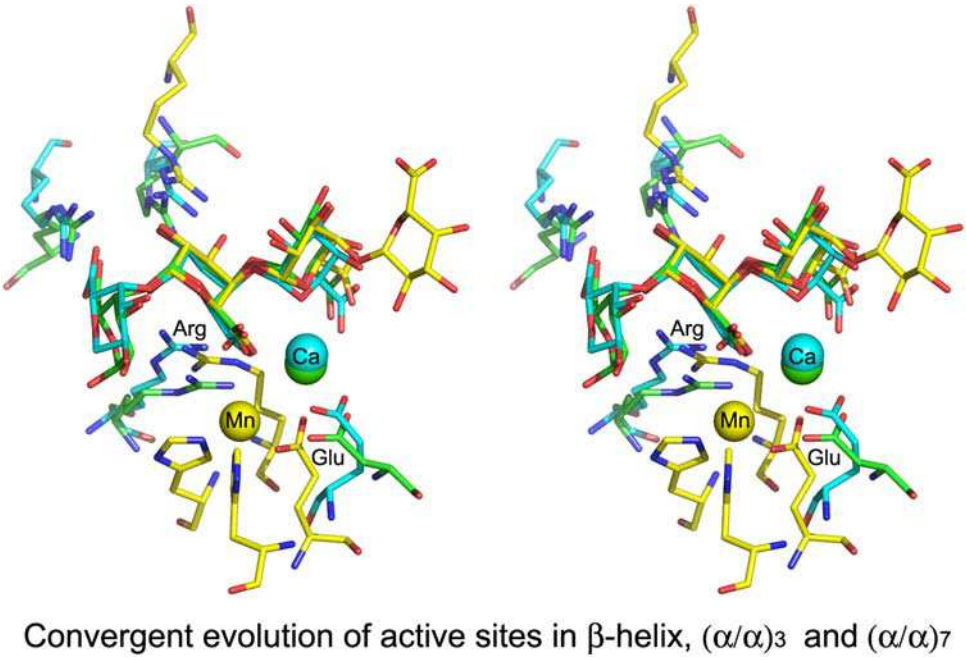

Fig. 10. The convergent evolution of active sites in β-helix (PDB code 2EWE, cyan backbone), $(\alpha/\alpha)_3$ (PDB code 1GXO, green backbone), and $(\alpha/\alpha)_7$ (PDB code 2V8K, yellow backbone) folds. In each case, an arginine (marked Arg) plays the role of the Brønsted acid maintaining similar position of its guanidinium group relative to the +1 sugar despite approaching from different directions. The Ca^{2+} (or Mn^{2+} in case of 2V8K) neutralizes the acidic moiety of +1 sugar approaching from different sides.

ses: $(\alpha/\alpha)_4$ barrel, the multidomain $(\alpha/\alpha)_{5,6}$ toroid, the β-jelly roll, the triple-stranded β-helix, and (likely) the β-sandwich (Table IV). Interestingly, there is a correlation between the type of substrate and the mechanism of a corresponding lyase that depolymerizes this substrate. Pectin/pectate degradation is associated exclusively with metal-assisted mechanism while all other polysaccharides for which the enzymatic mechanisms have been worked out are processed by lyases utilizing the Tyr/His mechanism (Table V). DS is an exception, in that enzymes utilizing either mechanism are known: ChonB utilizes a Ca^{2+}-dependent mechanism while ChonABC employs a His/Tyr-dependent mechanism. The mechanism utilized by several families is still not fully characterized. These include RLs from PL4 and PL11, alginate and glucuronan lyases from PL14, and oligogalacturonan lyases from PL22. Nevertheless, all these lyases are likely associated with metal-assisted mechanism because a metal ion was found in their putative active sites.

Calcium-assisted β-elimination

Enzymatic studies of lyases from several PL families showed that the presence of calcium increases enzymatic activity, therefore raising the question of its role in catalysis. As mentioned above, only some enzymes utilize a Ca^{2+} ion(s) in their active sites and it is plausible that a more general role for calcium is to neutralize the highly negatively charged lyase substrates. Structural studies identified families PL1, PL2, PL3, PL6, PL9, PL10, PL11, and PL22 as requiring metal ions to neutralize the acidic group of the uronic acid (Table I).

The β-Helix Class. We will discuss the active site in this class using the *E. chrysanthemi* PelC structure (PDB code 1AIR) as a prototype of this fold (Scavetta et al. 1999). PelC utilizes up to four Ca^{2+} ions to help bind the pectate substrate. Other Pels employ fewer Ca^{2+} ions for this purpose. The calcium ions bound to PelC neutralize the negative charge of the polyGalA substrate resulting from the presence of the carboxylic groups. Ca^{2+} ions Ca1, Ca2, and Ca3 (Figure 8) are on the same side of the substrate oligosaccharide and are coordinated by sidechains from an acidic patch constituted by six amino acids (Asp129, Asp131, Asp160, Asp162, Asp170, and Glu166). Calcium Ca4 has fewer contacts and appears to have partial occupancy suggesting its lesser importance. The side of the polyGalA substrate opposite to the Ca^{2+} ions interacts with three basic amino acids, Lys172, Arg223, and Arg245. The carboxylic group of the sugar in the +1 position is neutralized by interaction with Ca^{2+} ions Ca2 and Ca3 and with Lys190. In the PelC structure, only Arg218 is well positioned to be the Brønsted base (Figure 8) and, indeed, mutation of this residue to a lysine inactivates the enzyme (Herron et al. 2003). Moreover, this arginine is strictly conserved through the PL1 family, and although unusual in the role of a proton acceptor, its function is consistent with the optimal pH for pectate lyases of between eight and nine. The role of an arginine as a general base is not unique to pectate lyases but has also been observed in several other enzymes including IMP dehydrogenase, fumarate reductase, and L-aspartate oxidase (Guillen Schlippe and Hedstrom 2005). As no other residues are in sufficiently close proximity to the bridging O4 oxygen between −1 and +1 sugars, a water molecule is the most likely the proton donor. In other PL1 pectate lyases, the three main calcium sites are well conserved, although some variations occur in the arrangement of amino acids around the Ca2 site. Of the residues

forming the basic patch in PelC, only Arg223, which hydrogen bonds with the C-3 and C-4 hydroxyl groups of the sugar in the +1 subsite, is conserved in PL1 family, suggesting that these interactions are important for proper orientation of the substrate in the active site.

Interestingly, the Ca^2-assisted mechanism is not fully conserved in all enzymes of the PL1 family. Several sequences of eukaryotic pectin lyases eliminate the need for Ca^{2+} ions by introducing the guanidinium group of an arginine in an appropriate position to neutralize the charge of the acidic group of the substrate. Pectin is a highly methylated substrate, more susceptible to degradation (Abbott and Boraston 2008). In the active site of pectin lyases, the residues of the acidic patch involved in Ca^{2+} binding are not conserved, and the binding site is enriched in apolar sidechains, predominantly the aromatic residues, tryptophan and histidine (Mayans et al. 1997). This is consistent with the requirements introduced by the less polar, methylated pectin substrate. A Ca^{2+} ion does not bind in the active site of pectin lyases and instead an arginine sidechain, which replaces one of the Ca^{2+}-coordinating glutamates, neutralizes the acidic group of the uronic acid in the +1 subsite. This arginine corresponds to Arg176 in pectin lyase A (PelA), replacing the Ca^{2+} ligand Glu166 in PelC. However, the catalytic arginine that plays the role of a Brønsted base in PelC is strictly conserved in pectin lyases and, similarly, a water molecule most likely plays the role of a Brønsted acid.

A somewhat different active site has evolved in families PL3 and PL9. Pectate lyases from these two families have generally lower specific activity than PL1 pectate lyases (Roy et al. 1999; Creze et al. 2008). For example, Pel9A (PL9 family) is a constitutive pectate lyase that alerts bacteria to the presence of substrates and leads to the activation of the expression of other, more active degrading enzymes (Jenkins et al. 2004). These lyases utilize a lysine as a Brønsted base instead of an arginine playing this role in other families. PL9 members retain the Ca^{2+} ion for neutralization of the acidic group of the substrate, similar to other pectate lyases. Only one Ca^{+2} ion is present in the lyases from PL3 and PL9 families and it corresponds structurally to Ca2 in the PelC structure. This Ca^{2+} is located between the carboxylic groups of sugars in the −1 and +1 positions. In the PL9 family, four aspartate residues (Asp209, Asp233, Asp234, and Asp237) stabilize the calcium involved in neutralization of the +1 carboxylic group. Unfortunately, the available structures of lyases from family PL3 are without Ca^{2+} ion in the active site and, therefore, its exact position is uncertain (Creze et al. 2008). Nevertheless, Asp173, Asp195, and Glu194 present in PelI (PL3 family) form an acidic patch near the +1 sugar and are the likely ligands of Ca^{2+} ion. Superposition of representatives from PL3, PL9, and PL1 families based only on their substrates shows that the location of the crucial Ca^{2+} ions and the Brønsted base (Arg or Lys) is conserved among them. Therefore, the key residues in the metal-assisted mechanism are present in all these enzymes—the basic residue (Arg or Lys) playing the role of a Brønsted base, a water molecule acting as a Brønsted acid, and Ca^{2+} to neutralize the acidic group of the +1 sugar.

Whereas a link between the substrate and the enzymatic mechanism seems to be clear for the majority of PLs, the PL6 family presents an interesting exception. This small family (~20 sequences) contains alginate lyases and the only chondroitinase outside of the PL8 family, ChonB, specific for IdoA-containing DS. The PL6 family is the only lyase family associated with the Ca^{2+}-assisted mechanism that contains enzymes degrading substrates other than pectate/pectin. Moreover, all other enzymes cleaving the glycosidic bond next to IdoA use a different enzymatic mechanism (see below). In the ChonB structure, calcium is located in an acidic patch formed by Asn213, Glu243, and Glu245 and two water molecules. In addition to using calcium for charge neutralization, ChonB also utilizes a basic residue, Lys250, as the Brønsted base. However, unlike the other β-helix metal-assisted enzymes, it utilizes the sidechain of Arg271 as the Brønsted acid rather than a water molecule (Figure 9). The role of Arg271 was confirmed by mutagenesis (Michel et al. 2004). Although the overall fold of PL6 family lyases is the same as that of other β-helix lyases, the orientations of their substrates differ considerably and the location of the active site and Ca^{2+}-coordinating residues are not superposable with the other β-helix PLs.

The $(\alpha/\alpha)_{3/7}$ Toroid Class. Pectate lyases having an $(\alpha/\alpha)_{3/7}$ toroid fold belong to the PL2 and PL10 families and also utilize a metal-assisted mechanism. Whereas majority of the pectate lyases are extracellular enzymes, the PL2 family contains periplasmic and cytoplasmic enzymes (Rodionov et al. 2004). This difference in subcellular localization affects the type of metal involved in their catalytic activity. Experiments with PL2A from *Yersinia enterocolitica* with an $(\alpha/\alpha)_7$ toroid fold showed that Mn^{2+} rather than Ca^{2+} is a more effective cation for recovering activity following metal depletion by EDTA addition (Abbott and Boraston 2007). The structure of this enzyme has been determined bound to either Mn^{2+} ion or to trigalacturonic acid, and superposition of both these structures shows that Mn^{2+} binds opposite to the carboxylic group of the sugar in the +1 subsite. The Mn^{2+} is coordinated by His109, His172, Glu130, and three water molecules. Despite a different fold and different metal ion, the active site topology is very similar to that observed in β-helix fold PL1 enzymes (Abbott and Boraston 2007). Superposition of the active site residues of PelC(PL1) and Pel2A(PL2) based on the sugars in the +1 position shows spatial conservation of several residues: Glu130 of PL2A and Glu166 of PelC are involved in metal coordination while Arg272 of PL2A and Arg233 of PelC stabilize the C2 and C3 hydroxyl groups of the +1 sugar (Figure 10). The position of the Brønsted base is not strictly conserved but the guanidinium group of Arg171 of PL2A is in a similar position to that of Arg218 in PelC. In both cases, it is expected that a water molecule acts as the Brønsted acid.

Analysis of the active site of the polygalacturonic acid lyase Pel10Acm from *Cellvibrio japonicus* (PL10) belonging to the $(\alpha/\alpha)_3$ incomplete toroid fold shows that it also has spatial similarities to the enzymes from the PL1 family (Charnock et al. 2002). Superposition of Pel10Acm and PelC based on the positions of their +1 sugars of their respective substrates shows several structurally conserved amino acids (Figure 10). The Ca^{2+} site in Pel10Acm is very close to Ca2 in PelC and interacts in a similar way with the carboxylic groups of the −1 and +1 sugars. In both families, the Ca^{2+} ion is stabilized by a bidentate interaction with Asp451 in Pel10Acm and the corresponding Glu166 in PelC. This Ca^{2+} is roughly equidistant from both carboxylic groups and its interaction is completed by three

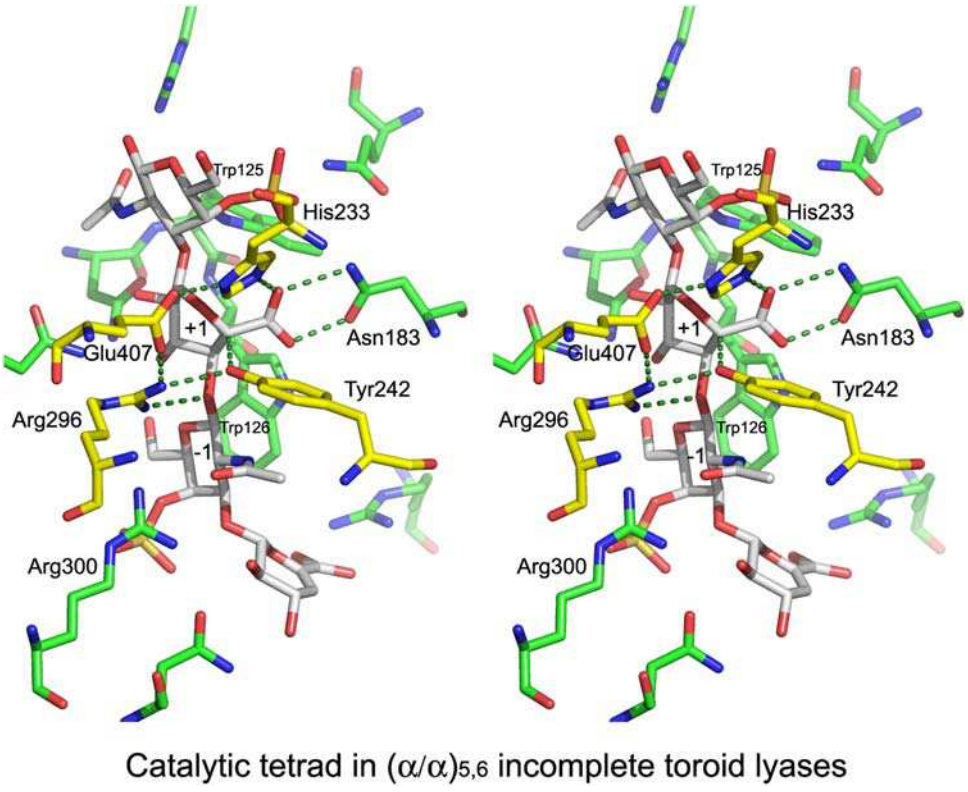

Fig. 11. The substrate-binding site and the catalytic tetrad in $(\alpha/\alpha)_{5,6}$ incomplete toroid lyases shown for *Arthrobacter aureus* ChonAC (PDB code 1RWH). The hydrogen bonds are marked by dashed lines. The active site tetrad is comprised of Tyr242, His233, Arg296, and Glu407 and is shown with carbon atoms colored yellow. The other residues surrounding the substrate are colored green, and the oligosaccharide is shown with gray carbon atoms. The neutralization of the acidic group of +1 sugar is accomplished by short hydrogen bonds between Asn183 and the acidic group of +1 sugar that promote its protonation.

water molecules. Pel10Acm also possesses an arginine, Arg524, in the same position as the Brønsted base Arg218in PelC. Based on the active site configuration of Pel10Acm, a water molecule is expected to be the Brønsted acid. In addition to catalytic amino acids, the basic patch formed by Arg610 and Arg625 in Pel10Acm corresponds to Arg223 and Arg245 in PelC.

These similarities in the active sites between pectate lyases belonging to three different folds, $(\alpha/\alpha)_3$ incomplete toroid, $(\alpha/\alpha)_7$ toroid, and β-helix, represent a clear example of a convergent evolution to a common active site employing a similar catalytic mechanism.

The β-Propeller Class. The enzymes with this fold belong to the PL11 and PL22 families. The structures of endo- and exo-RLs from PL11 family show the presence of two Ca^{2+} ions within the substrate binding cleft (Ochiai et al. 2009). The Ca^{2+} ions are coordinated by the Asp153 and Asn596 side-chains, the Ala594 and Asn592 main chain oxygens and two water molecules (site 1) and by His363, His399, Asp401, and Glu422 (site 2). The structures of several complexes with different sugars bound in the active site combined with molecular modeling led to the conclusion that the Ca^{2+} ions neutralize the carboxylic group of the +1 sugar (Ochiai et al. 2009). The nature of the other catalytic residues requires further investigation. Based on the comparison with other metal-dependent PLs, we propose that Lys535 or Arg452 could act as the Brønsted base.

In PL22 oligogalacturonan lyase, there is a Mn^{2+} situated at the open part of the β-propeller (PDB code 3C5M). This ion is stabilized by three histidines (His287, His353, and His355) and Gln350. This structural observation is in agreement with the observation that a related *E. chrysanthemi* lyase is more active in the presence of Mn^{2+} than Ca^{2+} (Shevchik et al. 1999). Based on metal-assisted mechanism used by all the pectate lyases, we hypothesize that, as in PL2, the Mn^{2+} ion would act as the neutralizer. Moreover, Arg349, situated in the vicinity of the Mn^{2+}-binding site, could play the role of a Brønsted base and a water molecule to be the Brønsted acid.

Histidine/tyrosine active site

Whereas the calcium-assisted mechanism is mainly associated with the β-helix fold, pectate lyases, and *anti* elimination, the His/Tyr mechanism is used by various enzymes acting on GlcA/IdoA-containing polysaccharides and by alginate lyases. The presence of C-5 epimers in the substrates is associated with the His/Tyr-containing active sites and indicates the ability of these lyases to perform both *anti* as well as *syn* elimination. Principally, two classes share this active site architecture, the multidomain $(\alpha/\alpha)_{4/5,6}$ toroid and the β-jelly roll. This active site topology appears to be more consistent between different folds than is the case with the calcium-assisted mechanism.

The $(\alpha/\alpha)_n$ Toroid Class. *The multidomain $(\alpha/\alpha)_n$ toroid subclass*—This subclass contains three families, PL8, PL15, and PL21. As described above, PL8 and PL21 families contain lyases that act on very similar substrates with GlcA or its C5 epimer IdoA in the +1 position, while PL15 lyases act on alginate. In the PL8 family, except for ChonABC, all enzymes

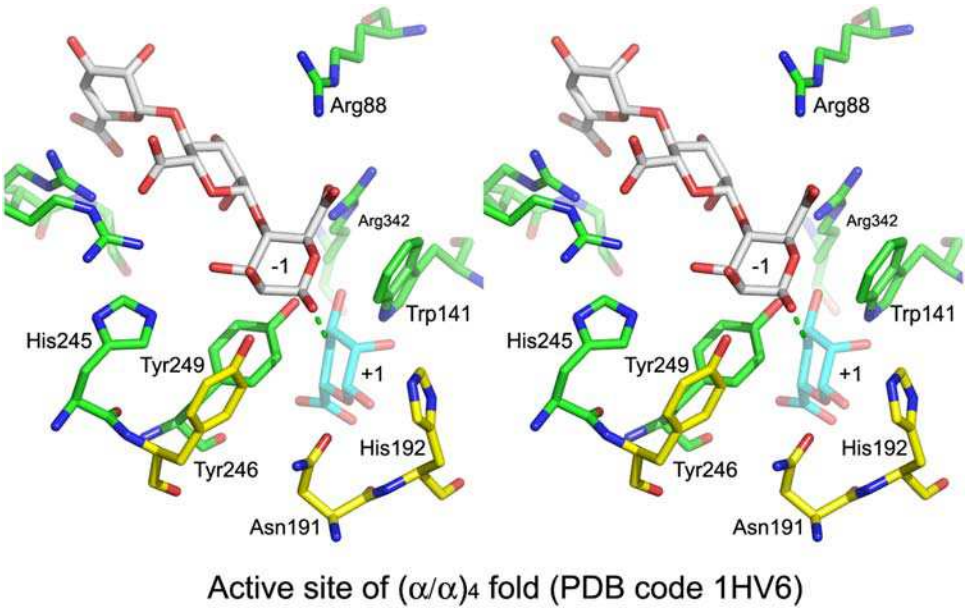

Fig. 12. Active site of $(\alpha/\alpha)_4$ fold PL (PDB code 1HV6). The trisaccharide present in the structure occupies "−1, −2, and −3" subsites. We have positioned approximately the sugar in +1 subsite (semi-transparent with cyan backbone). Tyr246 was proposed to act as the base and the acid, Asn191 was proposed to neutralize the acidic group, and His192 stabilizes the system. These three residues are colored yellow.

cleave (1-4) bond linking glucuronic acid to hexosamine (galactosamine for ChonAC, glucosamine for HL, and mannose for XL) performing *syn* elimination. ChonABC is a unique enzyme that can digest CS (e.g. GlcA) as well as DS (e.g. IdoA). Four amino acids (Tyr-His-Arg-Glu) involved in the catalytic mechanism have been identified (Figure 11) (Féthière et al. 1999; Li et al. 2000; Huang et al. 2001). This tetrad is strictly conserved within the PL8 family. A role for the Brønsted base has been suggested either for a histidine (Li et al. 2000) or for a tyrosine (Huang et al. 2001). The high resolution structure of *Arthrobacter aurescens* ChonAC clearly identified tyrosine in the appropriate distance and orientation to serve as the proton abstracting base (Figure 11) (Lunin et al. 2004). The same tyrosine also plays the role of a Brønsted acid. The dual role of the tyrosine in the catalytic mechanism of chondroitinase AC was further confirmed by kinetic studies (Rye et al. 2006). Moreover, deuterium kinetic isotope experiments showed that the deprotonation is the rate-limiting step of the reaction and suggested a step-wise rather than concerted mechanism (Rye and Withers 2002). The histidine is protonated and, together with a conserved asparagine, neutralizes the charge on the acidic group of the +1 glucuronic acid enabling the elimination reaction. The presence of two hydrogen bonds between the asparagine sidechain and the acidic group, found in the high resolution crystal structure, suggests strongly that the acidic group of GlcA is protonated in the enzyme-bound state. The neutralization of the acidic group by these enzymes is therefore accomplished not by a proximal positive charge but by forcing protonation of the acid. Another feature of these enzymes, extrapolated from the structure of ChonAC, is that the binding of the substrate forces the +1 GlcA into a twist-boat conformation (Figure 11), likely decreasing the activation energy barrier for the reaction by forcing the substrate to adopt a conformation closer to that of the transition state (Lunin et al. 2004).

The same catalytic tetrad as in ChonAC and HLs is also present in xanthan lyases (Maruyama et al. 2005) and in ChonABC (Huang et al. 2003; Shaya, Hahn, Park et al. 2008). Analysis of the structure of the *Bacillus* sp. GL1 xanthan lyase with oligosaccharides and the effect of mutagenesis on enzyme activity led to the proposal of a similar mechanism to that described above (Maruyama et al. 2005). Although no structure of ChonABC with a bound oligosaccharide is available, the importance of the tetrad for catalysis was confirmed by mutagenesis (Prabhakar et al. 2005; Shaya, Hahn, Park et al. 2008). It was proposed that neutralization of the acidic group of GlcA in the +1 subsite is accomplished by an aspartate sidechain, replacing the asparagine present in ChonAC, and requires its protonation (Shaya, Hahn, Bjerkan et al. 2008). The digestion of CS by ChonABC is likely performed in the same manner as in ChonAC, i.e. tyrosine serves both as the Brønsted base and acid (Shaya, Hahn, Park et al. 2008). The degradation of DS containing IdoA (*anti* elimination) has been proposed to involve His345 as a Brønsted base and its role in catalysis was confirmed by mutagenesis (Shaya, Hahn, Park et al. 2008). This histidine is located on the opposite side of the wide substrate binding cleft relative to the tetrad. The role of a Brønsted acid would be performed by the tyrosine from the tetrad. The role of His345 in catalysis was confirmed by mutagenesis (Shaya, Hahn, Park et al. 2008). Both DS and CS substrates use the same binding site but utilize different amino acids in the role of Brønsted base, with the active sites for these two substrates partially overlapping.

HepII, constituting PL21 family, possesses a similar ability as ChonABC to perform *syn* as well as *anti* elimination reactions: GlcA-containing HS and IdoA-containing heparin. The catalytically essential residues are Tyr257 and two histidines, His202 and His406. For the IdoA-containing substrate, it was proposed that His406 acts as a Brønsted base and Tyr257 performs as a Brønsted acid, while for GlcA-containing substrate Tyr257 per-

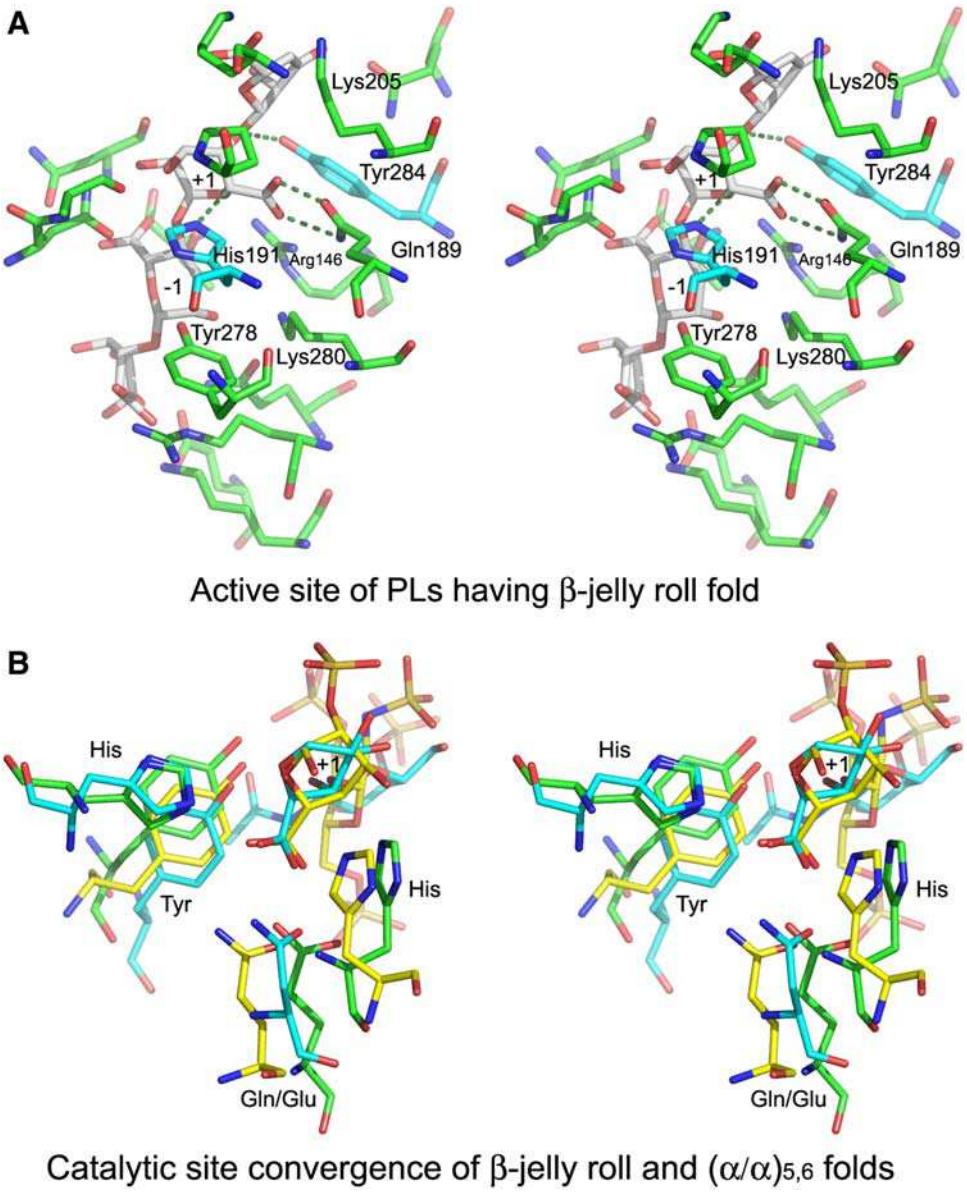

Fig. 13. Active site of PLs having β-jelly roll fold. (**A**) Alginate lyase A1-II′ with a tetrasaccharide substrate (PDB code 2ZAA). The two residues, Tyr284 and His191, mutated in this structure were restored from coordinates in 2Z42 and 2ZAB (colored in magenta); (**B**) convergence of the catalytic site geometry of the β-jelly roll and the $(\alpha/\alpha)_{5,6}$ fold PLs. The superposition of essential residues of β-jelly roll *B. thetaiotaomicron* HepI (yellow carbons, PDB code 3ILR) with $(\alpha/\alpha)_{5,6}$ *A. aurescens* ChonAC (cyan carbons, PDB code 1RWH) and HepII (green carbons, PDB code 2FUT) based on the positions of their +1 sugars. The histidines are present on both sides of the sugar in HepII but only on one side in the other two enzymes. This correlates with their sugar epimer specificity.

forms both functions. His202 is likely helping in neutralization of the negative charge of the acidic group of the uronic acid (Shaya et al. 2006). Interestingly, neutralization of the acidic group is accomplished by interaction with Glu205, implying protonation of one of these acidic groups. Glu205 is flanked by Arg261, which is also hydrogen bonded to the acidic group of the substrate, assisting the charge neutralization. Both HepII and ChonABC, the broad substrate-specificity enzymes, display yet another remarkable similarity by using an acidic residue (Glu/Asp) for charge neutralization instead of the amides (Gln/Asn) found in their stringent substrate-specific counterparts HepI and ChonAC.

Atu3025 (PL15 family) is the first structure of exolytic alginate lyase (Ochiai et al. 2010). Even though Atu3025 acts on a different substrate than PL8 and PL21 lyases, it retains high similarity of the catalytic residues with other lyases belonging to this subclass. The superposition of Atu3025 and HepII (PDB code 3AFL and 2FUT, respectively) guided by the positions of their bound substrates showed that Tyr365, His311, and His531 in Atu3025 overlap with Tyr257, His202, and His406 in HepII. In addition to the conservation of catalytic residues, several other residues in the substrate-binding site are conservatively replaced, namely Glu254, Asp416, Tyr555, and Phe558 in Atu3025 correspond to Asp145, Asp307, Tyr429, and Tyr436

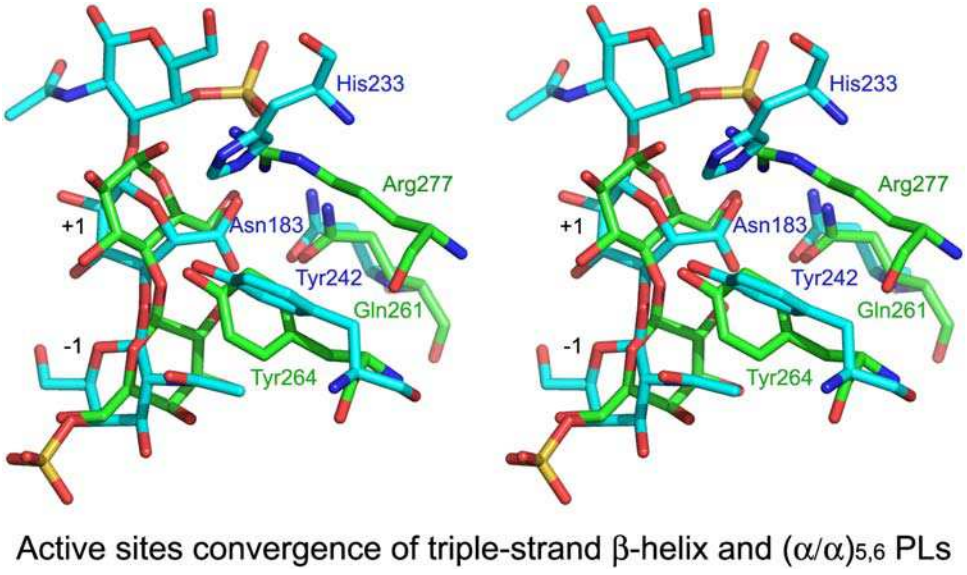

Fig. 14. Superposition of active sites of triple-stranded β-helix (PDB code 2YVV, green backbone) and $(\alpha/\alpha)_{5,6}$ (PDB code 1RWH, cyan backbone) fold PLs suggesting convergence of their active sites. This superposition shows that +1 sugar, asparagine (neutralization), and tyrosine in both folds are in similar relative positions. The position of the imidazole of the histidine in the $(\alpha/\alpha)_{5,6}$ fold is occupied by the guanidinium moiety of an arginine in the triple helix fold.

in HepII. Interestingly, Glu205 that played the role of neutralizer of acidic group of +1 sugar in HepII is not conserved in Atu3025 and is replaced by Arg314. Based on these observations, we hypothesize that in Atu3025, Tyr365 would play a role of the Brønsted acid while either Tyr365 or His311 acts as the Brønsted base depending on the epimer of the substrate. The neutralization would occur via a completely different interaction system involving Arg314 and Ser310.

The $(\alpha/\alpha)_4$ incomplete toroid subclass—This fold is found only in the PL5 family, which contains sequences annotated as alginate lyases (CAZy (Cantarel et al. 2009)). Only one structure of a lyase from this family is presently known, that of the alginate lyase A1-III (PDB code 1HV6) (Yoon et al. 2001). The roles of the Brønsted acid and base have been assigned to the same residue, Tyr246, while the neutralization of the acidic group of the +1 sugar has been postulated to occur through the hydrogen bonding to Asn191 with the possible assistance of His192 on one side and Glu236 and Arg239 on the other side (Figure 12) (Yoon et al. 2001). Comparing the $(\alpha/\alpha)_{5,6}$ and the $(\alpha/\alpha)_4$ toroid fold enzymes, their active sites are only partially superposable, with the key tyrosines and asparagines coming from the same secondary structural elements, while the other sidechains involved in the catalysis occupy similar positions but are at different locations in their respective sequences.

The β-Jelly Roll Class. This class contains enzymes from five PL families that degrade alginate, heparin, and glucuronan. Heparin (IdoA-rich) and guluronate sugars of alginate have the same configuration at the C-5 of the hexouronate, with the acidic group being on the same side of the ring in both polysaccharides. The mannuronate sugar of alginate has the same configuration at C-5 as GlcA (HS). Despite a conservation of the active site architecture within this fold, both *syn* and *anti* elimination mechanisms are observed; HepI (PL13) acts by *anti* elimination, guluronan lyases (PL20) by *syn* elimination, whereas some alginate lyases (PL7 and PL18) act by *anti* as well as *syn* elimination and depolymerize polyG and polyM tracts within the alginate polymer. The active sites have been identified for enzymes from four families, PL7, PL13, PL18, and PL20, but not yet for the family PL14. The latter is structurally most distant from the others. The residues involved in catalysis are conserved within the first three PL families. These are, in the case of HepI as an example, Tyr357 acting as a Brønsted acid, His151 is a Brønsted base, Gln149 and Arg83 are neutralizing the acidic group of the +1 sugar with Glu85 tying the latter two residues together by hydrogen bonds (Han et al. 2009) (Figure 13A). In addition to the conservation of active site residues, the enzymes from these three PL families share a number of other residues in their substrate-binding sites (Ile146, Tyr351, Phe352, Lys353, and Gly355 of HepI (PL13) correspond to Ile186, Tyr278, Phe279, Lys280, and Gly282 in A1-II′ (PL7) and to Ile87, Tyr180, Phe181, Lys182, and Gly184 in alginate lyase from *Pseudoalteromonas* sp. 272 (PL18)). This conservation indicates a more recent common ancestor. Although the active sites of these enzymes are conserved, HepI can only cleave the bond next to the IdoA sugar. It would appear that alginate lyases may be able to utilize the tyrosine not only as a Brønsted acid but also as a Brønsted base, depending on the type of elimination *syn* or *anti*, while HepI is unable to do so. This may be related to its inability to appropriately orient the GlcA sugar in the context of HS within its active site. Although the PL18 alginate lyase depolymerizes both polyM and polyG substrates, it displays higher activity for guluronate (G) oligomers (Iwamoto et al. 2001).

The structure of *Trichoderma reesei* glucuronan lyase from family PL20 (PDB code 2ZZJ (Konno et al. 2009)) diverges from the above set of active site residues. It has retained a glutamine (Gln91) that neutralizes the acidic group and the tyrosine (Tyr200) as an active site residue. However, the second

Table VI. PL families grouped by catalytic mechanism

PL	Enzyme	Fold	*syn/anti*	Base	Acid	Neutralizer
3	Pectate lyase	β-Helix (8 turns)	*anti*	Lys	H_2O	Ca^{2+}
1	Pectate lyase Exo-pectate lyase Pectin lyase	β-Helix (10 turns)	*anti* *anti* *anti*	Arg Arg	H_2O H_2O	Ca^{2+} Arg
9	Pectate lyase Exopolygalacturonate lyase	β-Helix (11 turns)	*anti* *anti*	Lys	H_2O	Ca^{2+}
6	Alginate lyase Chondroitinase B	β-Helix (14 turns)	*anti/syn* *anti*	Lys	Arg	Ca^{2+}
11	Rhamnogalacturonan lyase	β-Propeller (eight-bladed)	*anti*	N.D.	N.D.	Ca^{2+}
22	Oligogalacturonan lyase	β-Propeller (seven-bladed)	*anti*	N.D.	N.D.	Mn^{2+}
10	Pectate lyase	$(\alpha/\alpha)_3$ Barrel	*anti*	Arg	H_2O	Ca^{2+}
2	Pectate lyase	$(\alpha/\alpha)_7$ Barrel	*anti*	Arg	H_2O	Mn^{2+}
5	Alginate lyase	$(\alpha/\alpha)_4$ Barrel	*syn/anti*	Tyr/His	Tyr	Asn
8	Chondroitinase AC Xanthan lyase Hyaluronate lyase Chondroitinase ABC	$(\alpha/\alpha)_{5,6}$ Barrel + antiparallel β-sandwich + N-terminal antiparallel β-sandwich	*syn* *syn* *syn* *syn/anti*	Tyr/His	Tyr	Asx
21	Heparinase II	$(\alpha/\alpha)_{5,6}$ Barrel + antiparallel β-sandwich	*syn/anti*	Tyr/His	Tyr	Glu
15	Oligo-alginate lyase	$(\alpha/\alpha)_{5,6}$ Barrel + antiparallel β-sandwich	*syn/anti*	Tyr/His	Tyr	Arg
13	Heparinase I	β-Jelly roll	*anti*	His	Tyr	Gln
18	Alginate lyase	β-Jelly roll	*syn/anti*	Tyr/His	Tyr	Gln
7	Alginate lyase α-L-Guluronate lyase	β-Jelly roll	*syn/anti*	Tyr/His	Tyr	Gln
20	Endo-β-1,4-glucuronan lyase	β-Jelly roll	*syn*	Tyr	Tyr	Gln
14	Alginate lyase	β-Jelly roll	*syn/anti*	N.D.	N.D.	N.D.
16	Hyaluronan lyase	Triple-stranded β-helix	*syn*	Arg	Tyr	Gln
NC	K5 lyase (heparosan lyase)	Triple-stranded β-helix	*syn*	Lys	Lys	Glu
4	Rhamnogalacturonan lyase	3 β-Sandwich domains	*anti*	N.D.	N.D.	N.D.
12	Heparinase III	N.D.	*syn*	N.D.	N.D.	N.D.
17	Alginate lyase	N.D.	*anti*	N.D.	N.D.	N.D.

neutralizing residue, arginine, is replaced by His53 and, what is surprising, the histidine acting as a Brønsted base in HepI is replaced by Ile93 (Konno et al. 2009). The lack of conservation of this histidine is related to the configuration of the C-5 acidic group in glucuronic acid, which would in this case point toward Ile93, while the proton would be on the other side of the sugar ring, facing Tyr200. Therefore, it is most likely that Tyr200 fulfills a dual role as the Brønsted acid and Brønsted base, making the similar *syn* elimination to those of chondroitin and HLs having $(\alpha/\alpha)_{5,6}$ fold. Indeed, inspection of the active sites of these enzymes shows that, despite very different folds, their key catalytic residues can be superimposed relative to the substrate indicating convergent evolution (Figure 13B).

Even more extended convergent evolution between the $(\alpha/\alpha)_{5,6}$ and β-jelly roll folds becomes apparent by comparing PL7 alginate lyases and PL13 HepI lyase with PL21 HepII lyase. All these lyases can degrade substrates containing mannuronate or IdoA sugars and utilize the same His/Tyr mechanism. Their active sites show very similar arrangement of identical catalytic residues (Han et al. 2009). We find that this conservation also

extends to the active site residues involved in the degradation of this sugar epimer. For example, residues Tyr357 and His151 of HepI can be superposed with Tyr257 and His202 of HepII. To neutralize the carboxylic group of +1 sugar, HepI utilizes Gln149 while HepII uses Glu205 and Arg261, which together also cause the protonation of the acidic group on the sugar. The residue His406 of HepII that is essential for GlcA degradation is not conserved in HepI as this sugar is not a substrate of HepI.

The alginate lyase from family PL14 shows the same overall fold; however, none of the above mentioned residues are present in this enzyme (Ogura et al. 2009). The substrate-binding site extending along the inner β-sheet is closed by loops from opposite directions than in the previously described proteins. Two residues that were identified by mutagenesis as catalytically important, Lys197 and Ser219, are located at the opposite end of the substrate-binding site as compared to HepI. Although there are three tyrosine residues in the vicinity of the bound monosaccharide, their mutation has little effect on activity. It is therefore likely that the bound sugar occupies neither +1 nor −1 subsite but a subsite further away from the active site. The detailed mechanism of this enzyme has yet to be worked out.

Triple-Stranded β-Helix. The active site of this phage-encoded HL has been postulated on the basis of its complex with lactose, which mimics the product. The substrate-binding site is within a long groove on the protein surface that extends parallel to the β-helix axis. The key catalytic residue is Tyr264, which is proposed to play the role of a Brønsted acid, while Arg279 (or possibly the same Tyr264) is a putative Brønsted base (Mishra et al. 2009). The neutralization of the acidic group of +1 GlcA sugar of HA is proposed to be performed by Gln261. The importance of Tyr264 for catalysis was confirmed by mutagenesis (Mishra et al. 2009). We have compared the active site of this phage HL with that of bacterial HLs and ChonAC (Figure 14). Structural superposition of the lactose and oligosaccharide in the respective enzyme-binding sites shows that the position of Tyr264 is very close to that of the active site Tyr of the $(\alpha/\alpha)_{5,6}$ fold enzymes and that the Gln261 is close to the Asn that neutralizes the carboxylic group of +1 uronic acid. As well, Arg279 of phage HL is in close proximity to the His of the tetrad. The spatial arrangement of the three putative active site residues in phage HL relative to the substrate is therefore very similar to that observed in $(\alpha/\alpha)_{5,6}$ fold enzymes. This is yet another example of the convergent evolution of an active site embedded within two different PL folds.

The active site in KflA lyase has been identified as containing Glu206 and Lys208. Interestingly, the spatial arrangement of KflA active site shows similarity to the active site ofd HepII, namely Glu206 and Lys208 superimpose well with Glu205 and Tyr257 of HepII. The proposed mechanism has Glu206 acting as a neutralizer of the acidic group forcing its protonation, and Lys208 would perform the dual base–acid role, as a tyrosine in other *syn* elimination lyases (Thompson et al. 2010).

The β-Sandwich Class. These enzymes belong to the PL4 family. Only one structural representative is known for this fold, that of RL (RhgB) from *Aspergillus aculeatus* KSM 510 (McDonough et al. 2004). This protein contains three domains with the N- and C-terminal domains packing tightly together. No complex with a substrate or product has been determined so far. Nevertheless, the analysis of related sequences indicates that Lys150, Tyr203, Tyr205, and His210 in the N-terminal domain are strictly conserved. In addition, Arg451 and Arg455 in the C-terminal domain are in close proximity. All of these residues are within a canyon in the protein surface and suggest a likely location for the substrate-binding site. No metal ion has been found in the vicinity of these conserved residues. We postulate that enzymes with this fold also utilize the Tyr/His mechanism.

Conclusion

Based on sequence similarity, PLs are classified into 21 different families. Analysis and comparison of their three-dimensional structures show that they can be divided into five structural classes. Several of the folds represented in PLs, namely $(\alpha/\alpha)_6$, β-jelly roll, β-helix, and β-propeller, are not restricted to lytic enzymes degrading polysaccharides but occur also among hydrolytic enzymes that process polysaccharides. On the other hand, the most common architecture among the GHs, the TIM barrel fold (Cantarel et al. 2009), has not been yet found among PLs.

Whatever the architecture, only two different enzymatic mechanisms evolved for β-elimination. The first mechanism utilizes a metal-assisted neutralization of the acidic group on the substrate and occurs mainly in galacturonan lyases (pectate/pectin and RLs). The architecture of the active site of lyases with this mechanism is somewhat flexible with regard to active site organization and its amino acid composition. The function of a Brønsted base is usually adopted by an arginine or a lysine residue and the Brønsted acid is frequently a water molecule. This mechanism is found in the β-helix class, $(\alpha/\alpha)_{3/7}$ toroid class, and β-propeller class.

The second mechanism utilizes Asx/Glx to neutralize the acidic group of the substrate, a Tyr or His as a Brønsted base and a Tyr as a Brønsted acid. This mechanism is utilized by enzymes belonging to the multidomain $(\alpha/\alpha)_{4/5,6}$ toroid and β-jelly roll classes. It appears that the active site associated with this mechanism can accommodate both epimers of the uronic acid as shown by ChonABC and HepII, which can cleave the bond next to glucuronic acid or iduronic acid, and alginate lyases, which can act on guluronic acid and mannuronic acid within the alginate polymer. For example, the PL7 family alginate lyase A1-II′ from *Sphingomonas* sp. A1 can cleave poly(M), poly(G), or poly(MG) polysaccharides while others are more specific, e.g. the guluronate lyase alyPG from *Corynebacterium* sp. cleaves only Poly(G).

Table VI grouped the PL families based on their catalytic mechanism. That only two implementations of the general chemical mechanism are found in nature and have been reinvented in different folds (convergent evolution) indicates that these are robust chemical solutions that can be established within multiple architectures and adopted to process different substrates. The data in Table VI also show clearly that the use of the same sidechain as a Brønsted base and acid (Tyr) is only possible in the case of enzymes degrading polysaccharide substrates in which the C-5 proton and the O-4 oxygen of the

acidic hexose are in a *syn* configuration. The prevalence of pectate/pectin lyases with the β-helix fold and the association of this substrate with the metal-assisted mechanism indicate an interplay between the conformational requirements of the substrate and the fold that can accommodate these requirements.

Acknowledgments

We would like to thank Dr. David Shaya for assembling initial data for this review, Drs. Robert J. Linhardt, Allan Matte, and B. Henrissat for critically reading the manuscript and providing insightful comments. We are also thankful to the reviewers whose comments were extremely helpful. This work was supported in part by Canadian Institutes for Health Research grant GSP-48370 to MC.

Conflict of interest statement

None declared.

Abbreviations

ChonABC, chondroitin lyase ABC; ChonAC, chondroitin lyase AC; ChonB, chondroitin lyase B; CS, chondroitin sulfate; DS, dermatan sulfate; GAG, glycosaminoglycan; GH, glycoside hydrolase; GT, glycosyltransferase; HA, hyaluronic acid; HepI, heparinase I; HepII, heparinase II; HepIII, heparinase III; HL, HA lyase; HS, heparan sulfate; PelC, pectate lyase C; PGA, polygalacturonan; PL, polysaccharide lyase; RG, rhamnogalacturonan; RL, rhamnogalacturonan lyase; TSP, tail spike protein.

References

Abbott DW, Boraston AB. 2007. A family 2 pectate lyase displays a rare fold and transition metal-assisted beta-elimination. *J Biol Chem*. 282:35328–35336.

Abbott DW, Boraston AB. 2008. Structural biology of pectin degradation by Enterobacteriaceae. *Microbiol Mol Biol Rev*. 72:301–316.

Bertozzi CR, Kiessling LL. 2001. Chemical glycobiology. *Science*. 291: 2357–2364.

Boneca IG. 2005. The role of peptidoglycan in pathogenesis. *Curr Opin Microbiol*. 8:46–53.

Cantarel BL, Coutinho PM, Rancurel C, Bernard T, Lombard V, Henrissat B. 2009. The Carbohydrate-Active EnZymes database (CAZy): An expert resource for glycogenomics. *Nucleic Acids Res*. 37:D233–D238.

Capila I, Linhardt RJ. 2002. Heparin-protein interactions. *Angew Chem Int Ed*. 41:391–412.

Charnock SJ, Brown IE, Turkenburg JP, Black GW, Davies GJ. 2002. Convergent evolution sheds light on the anti-beta -elimination mechanism common to family 1 and 10 polysaccharide lyases. *Proc Natl Acad Sci USA*. 99: 12067–12072.

Chen D, Wu XZ, Wen ZY. 2008. Sulfated polysaccharides and immune response: Promoter or inhibitor? *Panminerva Med*. 50:177–183.

Cosgrove DJ. 1997. Assembly and enlargement of the primary cell wall in plants. *Annu Rev Cell Dev Biol*. 13:171–201.

Creze C, Castang S, Derivery E, Haser R, Hugouvieux-Cotte-Pattat N, Shevchik VE, Gouet P. 2008. The crystal structure of pectate lyase peli from soft rot pathogen Erwinia chrysanthemi in complex with its substrate. *J Biol Chem*. 283:18260–18268.

Cummings JH, Stephen AM. 2007. Carbohydrate terminology and classification. *Eur J Clin Nutr*. 61:S5–S18.

Davies GJ, Wilson KS, Henrissat B. 1997. Nomenclature for sugar-binding subsites in glycosyl hydrolases. *Biochem J*. 321:557–559.

DeAngelis PL. 2002. Evolution of glycosaminoglycans and their glycosyltransferases: Implications for the extracellular matrices of animals and the capsules of pathogenic bacteria. *Anat Rec*. 268:317–326.

DeAngelis PL, Gunay NS, Toida T, Mao WJ, Linhardt RJ. 2002. Identification of the capsular polysaccharides of Type D and F Pasteurella multocida as unmodified heparin and chondroitin, respectively. *Carbohydr Res*. 337: 1547–1552.

Ernst S, Langer R, Cooney CL, Sasisekharan R. 1995. Enzymatic degradation of glycosaminoglycans. *Crit Rev Biochem Mol Biol*. 30:387–444.

Esko JD, Selleck SB. 2002. Order out of chaos: Assembly of ligand binding sites in heparan sulfate. *Annu Rev Biochem*. 71:435–471.

Féthière J, Eggimann B, Cygler M. 1999. Crystal structure of chondroitin AC lyase, a representative of a family of glycosaminoglycan degrading enzymes. *J Mol Biol*. 288:635–647.

Fischer FG, Dorfel H. 1955. Polyuronic acids in brown algae. *Hoppe Seylers Z Physiol Chem*. 302:186–203.

Gabius HJ. 2000. Biological information transfer beyond the genetic code: The sugar code. *Naturwissenschaften*. 87:108–121.

Gabius HJ. 2006. Cell surface glycans: The why and how of their functionality as biochemical signals in lectin-mediated information transfer. *Crit Rev Immunol*. 26:43–79.

Gacesa P. 1987. Alginate-modifying enzymes. A proposed unified mechanism of action for the lyases and epimerases. *FEBS Lett*. 212:199–202.

Gagneux P, Varki A. 1999. Evolutionary considerations in relating oligosaccharide diversity to biological function. *Glycobiology*. 9:747–755.

Garcia-Ochoa F, Santos VE, Casas JA, Gomez E. 2000. Xanthan gum: Production, recovery, and properties. *Biotechnol Adv*. 18:549–579.

Guillen Schlippe YV, Hedstrom L. 2005. A twisted base? The role of arginine in enzyme-catalyzed proton abstractions. *Arch Biochem Biophys*. 433:266–278.

Han YH, Garron ML, Kim HY, Kim WS, Zhang Z, Ryu KS, Shaya D, Xiao Z, Cheong C, Kim YS, et al. 2009. Structural snapshots of heparin depolymerization by heparin lyase I. *J Biol Chem*. 284:34019–34027.

Hashimoto W, Miki H, Tsuchiya N, Nankai H, Murata K. 1998. Xanthan lyase of Bacillus sp. strain GL1 liberates pyruvylated mannose from xanthan side chains. *Appl Environ Microbiol*. 64:3765–3768.

Hashimoto W, Nankai H, Mikami B, Murata K. 2003. Crystal structure of Bacillus sp. GL1 xanthan lyase, which acts on the side chains of xanthan. *J Biol Chem*. 278:7663–7673.

Hashimoto W, Momma K, Maruyama Y, Yamasaki M, Mikami B, Murata K. 2005. Structure and function of bacterial super-biosystem responsible for import and depolymerization of macromolecules. *Biosci Biotechnol Biochem*. 69:673–692.

Henrissat B, Sulzenbacher G, Bourne Y. 2008. Glycosyltransferases, glycoside hydrolases: Surprise, surprise! *Curr Opin Struct Biol*. 18:527–533.

Herron SR, Scavetta RD, Garrett M, Legner M, Jurnak F. 2003. Characterization and implications of Ca2+ binding to pectate lyase C. *J Biol Chem*. 278: 12271–12277.

Heyraud A, Courtois J, Dantas L, Colin-Morel P, Courtois B. 1993. Structural characterization and rheological properties of an extracellular glucuronan produced by a Rhizobium meliloti M5N1 mutant strain. *Carbohydr Res*. 240:71–78.

Huang W, Boju L, Tkalec L, Su H, Yang HO, Gunay NS, Linhardt RJ, Kim YS, Matte A, Cygler M. 2001. Active site of chondroitin AC lyase revealed by the structure of enzyme-oligosaccharide complexes and mutagenesis. *Biochemistry*. 40:2359–2372.

Huang W, Lunin VV, Li Y, Suzuki S, Sugiura N, Miyazono H, Cygler M. 2003. Crystal structure of Proteus vulgaris chondroitin sulfate ABC lyase I at 1.9A resolution. *J Mol Biol*. 328:623–634.

Iozzo RV. 1998. Matrix proteoglycans: From molecular design to cellular function. *Annu Rev Biochem*. 67:609–652.

Iozzo RV, Zoeller JJ, Nystrom A. 2009. Basement membrane proteoglycans: Modulators Par Excellence of cancer growth and angiogenesis. *Mol Cells*. 27:503–513.

Iwamoto Y, Araki R, Iriyama K, Oda T, Fukuda H, Hayashida S, Muramatsu T. 2001. Purification and characterization of bifunctional alginate lyase from Alteromonas sp. strain no. 272 and its action on saturated oligomeric substrates. *Biosci Biotechnol Biochem*. 65:133–142.

Jackson RL, Busch SJ, Cardin AD. 1991. Glycosaminoglycans: Molecular properties, protein interactions, and role in physiological processes. *Physiol Rev*. 71:481–539.

Jenkins J, Mayans O, Pickersgill R. 1998. Structure and evolution of parallel beta-helix proteins. *J Struct Biol*. 122:236–246.

Jenkins J, Shevchik VE, Hugouvieux-Cotte-Pattat N, Pickersgill RW. 2004. The crystal structure of pectate lyase Pel9A from Erwinia chrysanthemi. *J Biol Chem*. 279:9139–9145.

Kjellen L, Lindahl U. 1991. Proteoglycans: Structures and interactions. *Annu Rev Biochem*. 60:443–475.

Knox JP. 2008. Revealing the structural and functional diversity of plant cell walls. *Curr Opin Plant Biol*. 11:308–313.

Knudson CB, Knudson W. 2001. Cartilage proteoglycans. *Semin Cell Dev Biol*. 12:69–78.

Kogan G, Soltes L, Stern R, Gemeiner P. 2007. Hyaluronic acid: A natural biopolymer with a broad range of biomedical and industrial applications. *Biotechnol Lett*. 29:17–25.

Konno N, Ishida T, Igarashi K, Fushinobu S, Habu N, Samejima M, Isogai A. 2009. Crystal structure of polysaccharide lyase family 20 endo-β-1,4-glucuronan lyase from the filamentous fungus Trichoderma reesei. *FEBS Lett*. 583:1323–1326.

Lairson LL, Henrissat B, Davies GJ, Withers SG. 2008. Glycosyltransferases: Structures, functions, and mechanisms. *Annu Rev Biochem*. 77:521–555.

Lauder RM. 2009. Chondroitin sulphate: A complex molecule with potential impacts on a wide range of biological systems. *Complement Ther Med*. 17: 56–62.

Li S, Kelly SJ, Lamani E, Ferraroni M, Jedrzejas MJ. 2000. Structural basis of hyaluronan degradation by *Streptococcus pneumoniae* hyaluronate lyase. *EMBO J*. 19:1228–1240.

Li S, Jedrzejas MJ. 2001. Hyaluronan binding and degradation by *Streptococcus agalactiae* hyaluronate lyase. *J Biol Chem*. 276:41407–41416.

Linhardt RJ. 2003. 2003 Claude S. Hudson Award address in carbohydrate chemistry. Heparin: Structure and activity. *J Med Chem*. 46:2551–2564.

Linhardt RJ, Avci FY, Toida T, Kim YS, Cygler M. 2006. CS lyases: Structure, activity, and applications in analysis and the treatment of diseases. *Adv Pharmacol*. 53:187–215.

Lunin VV, Li Y, Linhardt RJ, Miyazono H, Kyogashima M, Kaneko T, Bell AW, Cygler M. 2004. High-resolution crystal structure of *Arthrobacter aurescens* chondroitin AC lyase: An enzyme-substrate complex defines the catalytic mechanism. *J Mol Biol*. 337:367–386.

Macri L, Silverstein D, Clark RAF. 2007. Growth factor binding to the pericellular matrix and its importance in tissue engineering. *Adv Drug Deliv Rev*. 59:1366–1381.

Marth JD, Grewal PK. 2008. Mammalian glycosylation in immunity. *Nat Rev Immunol*. 8:874–887.

Maruyama Y, Hashimoto W, Mikami B, Murata K. 2005. Crystal structure of Bacillus sp. GL1 xanthan lyase complexed with a substrate: Insights into the enzyme reaction mechanism. *J Mol Biol*. 350:974–986.

Maruyama Y, Mikami B, Hashimoto W, Murata K. 2007. A structural factor responsible for substrate recognition by Bacillus sp. GL1 xanthan lyase that acts specifically on pyruvated side chains of xanthan. *Biochemistry*. 46: 781–791.

Mayans O, Scott M, Connerton I, Gravesen T, Benen J, Visser J, Pickersgill R, Jenkins J. 1997. Two crystal structures of pectin lyase A from *Aspergillus* reveal a pH driven conformational change and striking divergence in the substrate-binding clefts of pectin and pectate lyases. *Structure*. 5:677–689.

McCarter JD, Withers SG. 1994. Mechanisms of enzymatic glycoside hydrolysis. *Curr Opin Struct Biol*. 4:885–892.

McDonald JA, Camenisch TD. 2002. Hyaluronan: Genetic insights into the complex biology of a simple polysaccharide. *Glycoconj J*. 19:331–339.

McDonough MA, Kadirvelraj R, Harris P, Poulsen JC, Larsen S. 2004. Rhamnogalacturonan lyase reveals a unique three-domain modular structure for polysaccharide lyase family 4. *FEBS Lett*. 565:188–194.

Michel G, Pojasek K, Li Y, Sulea T, Linhardt RJ, Raman R, Prabhakar V, Sasisekharan R, Cygler M. 2004. The structure of chondroitin B lyase complexed with glycosaminoglycan oligosaccharides unravels a calcium-dependent catalytic machinery. *J Biol Chem*. 279:32882–32896.

Mishra P, Prem KR, Ethayathulla AS, Singh N, Sharma S, Perbandt M, Betzel C, Kaur P, Srinivasan A, Bhakuni V, et al. 2009. Polysaccharide binding sites in hyaluronate lyase—crystal structures of native phage-encoded hyaluronate lyase and its complexes with ascorbic acid and lactose. *FEBS J*. 276:3392–3402.

Miyazaki T, Yadomae T, Terui T, Yamada H, Kikuchi T. 1975. Studies on fungal polysaccharide. XVII. A new glucuronan "protuberic acid" produced by a fungus Kobayashia nipponica. *Biochim Biophys Acta*. 385:345–353.

Munoz EM, Linhardt RJ. 2004. Heparin-binding domains in vascular biology. *Arterioscler Thromb Vasc Biol*. 24:1549–1557.

Mutter M, Colquhoun IJ, Beldman G, Schols HA, Bakx EJ, Voragen AG. 1998. Characterization of recombinant rhamnogalacturonan alpha-L-rhamnopyranosyl-(1,4)-alpha-D-galactopyranosyluronide lyase from Aspergillus aculeatus. An enzyme that fragments rhamnogalacturonan I regions of pectin. *Plant Physiol*. 117:141–152.

Mythreye K, Blobe GC. 2009. Proteoglycan signaling co-receptors: Roles in cell adhesion, migration and invasion. *Cell Signal*. 21:1548–1558.

Ochiai A, Itoh T, Maruyama Y, Kawamata A, Mikami B, Hashimoto W, Murata K. 2007. A novel structural fold in polysaccharide lyases: Bacillus subtilis family 11 rhamnogalacturonan lyase YesW with an eight-bladed beta-propeller. *J Biol Chem*. 282:37134–37145.

Ochiai A, Itoh T, Kawamata A, Hashimoto W, Murata K. 2007. Plant cell wall degradation by saprophytic Bacillus subtilis strains: Gene clusters responsible for rhamnogalacturonan depolymerization. *Appl Environ Microbiol*. 73: 3803–3813.

Ochiai A, Itoh T, Mikami B, Hashimoto W, Murata K. 2009. Structural determinants responsible for substrate recognition and mode of action in family 11 polysaccharide lyases. *J Biol Chem*. 284:10181–10189.

Ochiai A, Yamasaki M, Mikami B, Hashimoto W, Murata K. 2010. Crystal structure of exotype alginate lyase Atu3025 from agrobacterium tumefaciens. *J Biol Chem*. 285:24519–24528.

Ogura K, Yamasaki M, Yamada T, Mikami B, Hashimoto W, Murata K. 2009. Crystal structure of family 14 polysaccharide lyase with pH-dependent modes of action. *J Biol Chem*. 284:35572–35579.

Ohtsubo K, Marth JD. 2006. Glycosylation in cellular mechanisms of health and disease. *Cell*. 126:855–867.

Parodi AJ. 2000. Protein glucosylation and its role in protein folding. *Annu Rev Biochem*. 69:69–93.

Prabhakar V, Raman R, Capila I, Bosques CJ, Pojasek K, Sasisekharan R. 2005. Biochemical characterization of the chondroitinase ABC I active site. *Biochem J*. 390:395–405.

Pritt B, O'Brien L, Winn W. 2007. Mucoid Pseudomonas in cystic fibrosis. *Am J Clin Pathol*. 128:32–34.

Redouan E, Cedric D, Emmanuel P, Mohamed el G, Bernard C, Philippe M, Cherkaoui el M, Josiane C. 2009. Improved isolation of glucuronan from algae and the production of glucuronic acid oligosaccharides using a glucuronan lyase. *Carbohydr Res*. 344:1670–1675.

Rehm BH, Valla S. 1997. Bacterial alginates: Biosynthesis and applications. *Appl Microbiol Biotechnol*. 48:281–288.

Rek A, Thompson J, Roberts IS, Kungl AJ. 2007. Biophysical investigation of recombinant K5 lyase: Structural implications of substrate binding and processing. *Biochim Biophys Acta*. 1774:72–77.

Remminghorst U, Rehm BH. 2006. Bacterial alginates: From biosynthesis to applications. *Biotechnol Lett*. 28:1701–1712.

Ridley BL, O'Neill MA, Mohnen D. 2001. Pectins: Structure, biosynthesis, and oligogalacturonide-related signaling. *Phytochemistry*. 57:929–967.

Roberts K. 1990. Structures at the plant cell surface. *Curr Opin Cell Biol*. 2: 920–928.

Rodionov DA, Gelfand MS, Hugouvieux-Cotte-Pattat N. 2004. Comparative genomics of the KdgR regulon in Erwinia chrysanthemi 3937 and other gamma-proteobacteria. *Microbiology*. 150:3571–3590.

Roughley PJ. 2006. The structure and function of cartilage proteoglycans. *Eur Cell Mater*. 12:92–101.

Roy C, Kester H, Visser J, Shevchik V, Hugouvieux-Cotte-Pattat N, Robert-Baudouy J, Benen J. 1999. Modes of action of five different endopectate lyases from Erwinia chrysanthemi 3937. *J Bacteriol*. 181:3705–3709.

Ruijssenaars HJ, Hartmans S, Verdoes JC. 2000. A novel gene encoding xanthan lyase of Paenibacillus alginolyticus strain XL-1. *Appl Environ Microbiol*. 66: 3945–3950.

Russell NJ, Gacesa P. 1989. Physicochemical properties of alginate from mucoid strains of Pseudomonas aeruginosa isolated from cystic fibrosis patients. *Antibiot Chemother*. 42:62–66.

Rye CS, Withers SG. 2002. Elucidation of the mechanism of polysaccharide cleavage by chondroitin AC lyase from Flavobacterium heparinum. *J Am Chem Soc*. 124:9756–9767.

Rye CS, Matte A, Cygler M, Withers SG. 2006. An atypical approach identifies TYR234 as the key base catalyst in chondroitin AC lyase. *Chembiochem*. 7:631–637.

Sarkar P, Bosneaga E, Auer M. 2009. Plant cell walls throughout evolution: Towards a molecular understanding of their design principles. *J Exp Bot*. 60:3615–3635.

Scavetta RD, Herron SR, Hotchkiss AT, Kita N, Keen NT, Benen JA, Kester HC, Visser J, Jurnak F. 1999. Structure of a plant cell wall fragment complexed to pectate lyase C. *Plant Cell*. 11:1081–1092.

Schaefer L, Schaefer RM. 2010. Proteoglycans: From structural compounds to signaling molecules. *Cell Tissue Res*. 339:237–246.

Scott JE. 2003. Elasticity in extracellular matrix 'shape modules' of tendon, cartilage, etc. A sliding proteoglycan-filament model. *J Physiol*. 553: 335–343.

Shaya D, Tocilj A, Li Y, Myette J, Venkataraman G, Sasisekharan R, Cygler M. 2006. Crystal structure of heparinase II from Pedobacter heparinus and its complex with a disaccharide product. *J Biol Chem*. 281:15525–15535.

Shaya D, Hahn BS, Park NY, Sim JS, Kim YS, Cygler M. 2008. Characterization of chondroitin sulfate lyase ABC from Bacteroides thetaiotaomicron WAL2926. *Biochemistry*. 47:6650–6661.

Shaya D, Hahn BS, Bjerkan TM, Kim WS, Park NY, Sim JS, Kim YS, Cygler M. 2008. Composite active site of chondroitin lyase ABC accepting both epimers of uronic acid. *Glycobiology*. 18:270–277.

Shevchik VE, Condemine G, Robert-Baudouy J, Hugouvieux-Cotte-Pattat N. 1999. The exopolygalacturonate lyase PelW and the oligogalacturonate lyase Ogl, two cytoplasmic enzymes of pectin catabolism in Erwinia chrysanthemi 3937. *J Bacteriol*. 181:3912–3919.

Smith NL, Taylor EJ, Lindsay AM, Charnock SJ, Turkenburg JP, Dodson EJ, Davies GJ, Black GW. 2005. Structure of a group A streptococcal phage-encoded virulence factor reveals a catalytically active triple-stranded beta-helix. *Proc Natl Acad Sci USA*. 102:17652–17657.

Steinbacher S, Seckler R, Miller S, Steipe B, Huber R, Reinemer P. 1994. Crystal structure of P22 tailspike protein: Interdigitated subunits in a thermostable trimer. *Science*. 265:383–386.

Stummeyer K, Dickmanns A, Muhlenhoff M, Gerardy-Schahn R, Ficner R. 2005. Crystal structure of the polysialic acid-degrading endosialidase of bacteriophage K1F. *Nat Struct Mol Biol*. 12:90–96.

Thompson JE, Pourhossein M, Waterhouse A, Hudson T, Goldrick M, Derrick JP, Roberts IS. 2010. The K5 lyase KflA combines a viral tail spike structure with a bacterial polysaccharide lyase mechanism. *J Biol Chem*. 285: 23963–23969.

Vlodavsky I, Ilan N, Nadir Y, Brenner B, Katz BZ, Naggi A, Torri G, Casu B, Sasisekharan R. 2007. Heparanase, heparin and the coagulation system in cancer progression. *Thromb Res*. 120(Suppl 2):S112–S120.

Withers SG, Madsen NB, Sykes BD, Takagi M, Shimomura S, Fukui T. 1981. Evidence for direct phosphate-phosphate interaction between pyridoxal phosphate and substrate in the glycogen phosphorylase catalytic mechanism. *J Biol Chem*. 256:10759–10762.

Yamada S, Sugahara K. 2008. Potential therapeutic application of chondroitin sulfate/dermatan sulfate. *Curr Drug Discov Technol*. 5:289–301.

Yamasaki M, Moriwaki S, Miyake O, Hashimoto W, Murata K, Mikami B. 2004. Structure and function of a hypothetical Pseudomonas aeruginosa protein PA1167 classified into family PL-7: A novel alginate lyase with a beta-sandwich fold. *J Biol Chem*. 279:31863–31872.

Yip VL, Withers SG. 2004. Nature's many mechanisms for the degradation of oligosaccharides. *Org Biomol Chem*. 2:2707–2713.

Yoder MD, Keen NT, Jurnak F. 1993. New domain motif: The structure of pectate lyase C, a secreted plant virulence factor. *Science*. 260:1503–1507.

Yoon HJ, Hashimoto W, Miyake O, Murata K, Mikami B. 2001. Crystal structure of alginate lyase A1-III complexed with trisaccharide product at 2.0 A resolution. *J Mol Biol*. 307:9–16.

Yoon JH, Halper J. 2005. Tendon proteoglycans: Biochemistry and function. *J Musculoskelet Neuronal Interact*. 5:22–34.